

Article

Metallothionein I/II Expression and Metal Ion Levels in Correlation with Amyloid Beta Deposits in the Aged Feline Brain

Emmanouela P. Apostolopoulou ¹ , Nikolaos Raikos ², Ioannis Vlemmas ¹, Efstratios Michaelidis ³ and Georgia D. Brellou ^{1,*} 

¹ Department of Pathology, Faculty of Health Sciences, School of Veterinary Medicine, Aristotle University of Thessaloniki, 54627 Thessaloniki, Greece; emmaapos@vet.auth.gr (E.P.A.); ivlemmas@vet.auth.gr (I.V.)

² Department of Forensic Medicine & Toxicology, Faculty of Health Sciences, School of Medicine, Aristotle University of Thessaloniki, 54124 Thessaloniki, Greece; raikos@auth.gr

³ Laboratories of the 3rd Army Veterinary Hospital, Chemical Department, 57001 Thessaloniki, Greece; mixeusart@yahoo.gr

* Correspondence: mprellou@vet.auth.gr; Tel.: +30-2310-994-530

Abstract: Brain aging has been correlated with high metallothionein I-II (MT-I/II) expression, iron and zinc dyshomeostasis, and A β deposition in humans and experimental animals. In the present study, iron and zinc accumulation, the expression of MT-I/II and A β 42, and their potential association with aging in the feline brain were assessed. Tissue sections from the temporal and frontal grey (GM) and white (WM) matter, hippocampus, thalamus, striatum, cerebellum, and dentate nucleus were examined histochemically for the presence of age-related histopathological lesions and iron deposits and distribution. We found, using a modified Perl's/DAB method, two types of iron plaques that showed age-dependent accumulation in the temporal GM and WM and the thalamus, along with the age-dependent increment in cerebellar-myelin-associated iron. We also demonstrated an age-dependent increase in MT-I/II immunoreactivity in the feline brain. In cats over 7 years old, A β immunoreactivity was detected in vessel walls and neuronal somata; extracellular A β deposits were also evident. Interestingly, A β -positive astrocytes were also observed in certain cases. ICP-MS analysis of brain content regarding iron and zinc concentrations showed no statistically significant association with age, but a mild increase in iron with age was noticed, while zinc levels were found to be higher in the Mature and Senior groups. Our findings reinforce the suggestion that cats could serve as a dependable natural animal model for brain aging and neurodegeneration; thus, they should be further investigated on the basis of metal ion concentration changes and their effects on aging.

Keywords: aging; feline; metallothionein I/II; iron; zinc; Perl's/DAB; amyloid beta; neurodegeneration; IHC; ICP-MS



Citation: Apostolopoulou, E.P.; Raikos, N.; Vlemmas, I.; Michaelidis, E.; Brellou, G.D. Metallothionein I/II Expression and Metal Ion Levels in Correlation with Amyloid Beta Deposits in the Aged Feline Brain. *Brain Sci.* **2023**, *13*, 1115. <https://doi.org/10.3390/brainsci13071115>

Academic Editors: Giuseppe Lupo and Maria Elena Miranda Banos

Received: 23 June 2023

Revised: 13 July 2023

Accepted: 19 July 2023

Published: 22 July 2023



Copyright: © 2023 by the authors. Licensee MDPI, Basel, Switzerland. This article is an open access article distributed under the terms and conditions of the Creative Commons Attribution (CC BY) license (<https://creativecommons.org/licenses/by/4.0/>).

1. Introduction

Advances in veterinary care and nutrition have led to significantly longer life expectancy for pet cats, with a reported median longevity of 14 years [1]. Aging is a biological phenomenon characterized by progressive and irreversible deterioration of physiological function, which eventually leads to age-related diseases. It has also been described as an important risk factor for many neurodegenerative diseases in humans, including Alzheimer's disease (AD) and Parkinson's disease (PD) [2]. The brain is probably the most vulnerable tissue affected by aging. The high oxygen requirement, iron storage capacity, elevated polyunsaturated fatty acid content, and low synthesis capacity of endogenous antioxidants, along with its limited regeneration capability, lead to increased brain vulnerability to oxidative stress [3]. Studies that have focused on aging in several animal species, such as cats, have described brain lesions comparable to those observed in human brain

aging and AD [4–8]. However, further research on age-related central nervous system (CNS) pathology is necessary to be conducted [4].

Common features of normal aging include increased blood–brain barrier permeability and glial senescence, which leads to age-dependent loss of function of neuroglia [9–12]. These changes might lead to the dysregulation of metal concentrations in the aging brain. Metal toxicity gives rise to oxidative stress, mitochondrial dysfunction, and DNA damage and may subsequently contribute to advanced aging and promote the onset of neurodegenerative diseases, such as AD and PD [13].

Iron is the most abundant essential trace metal in the brain and is vital for pleiotropic biological processes, including neurotransmitter synthesis, myelination of neurons, and mitochondrial function [14]. Similarly, zinc—the second most abundant metal in the brain—exerts modulatory effects on multiple cellular processes, such as neurotransmission, gene regulation, and enzymatic activity [15]. In normal aging, increased iron concentration can be observed in discrete brain regions: the substantia nigra, lentiform and caudate nuclei, globus pallidus, and cortices, in humans and mice [11,14,16]. Moreover, an age-dependent increase in zinc concentration has been reported in rats, humans, and mice [11]. Higher levels of iron and excessive zinc levels can trigger the generation of reactive oxygen species (ROS) [17]. Additionally, aging is associated with the inefficiency of antioxidant defense systems. Thus, elevated ROS concentrations evoke oxidative stress and lead to cell damage and eventually cell death [13,14,18]. Consequently, iron and zinc dyshomeostasis might play a critical pathophysiological role in age-related neurodegenerative diseases [13,14,19].

Taking into consideration the high zinc brain content in humans, the regulation of metal homeostasis is crucial [15]. Among other proteins, metallothioneins (MTs) are responsible for zinc regulation. They are small, cysteine-rich metal-binding proteins, which are present in most cells of the body, including several cell types in the brain and spinal cord [20]. Three MT isoforms are expressed in the mammalian brain: MT-I, MT-II, and MT-III. Of these, MT-I and MT-II (hereafter MT-I/II) have been considered equivalent proteins. They share similar expression profiles and structures, differing only by one amino acid and their ability to bind divalent metals, whereas they exert the same function [21]. Within the CNS, MT-I/II is mainly expressed in astrocytes, while other cell types also show MT-I/II expression, such as neurons, endothelial cells, leptomeningeal cells (LCs), ependymal cells, and CP epithelial cells [20–22]. Regarding brain aging, previous research has demonstrated elevated levels of MT-I/II in the astroglia of dogs, rats, and cattle [23–26]. Specifically, Mocchegiani and colleagues, in 2001, proposed MT-I/II as a potential marker of aging. Additionally, increased astroglial numbers are observed with age, and there is also a higher expression of astrocytic immunohistochemical markers, such as GFAP [2,4,11,14,27,28]. Earlier studies have demonstrated that high concentrations of zinc, copper, and iron are present in insoluble amyloid plaques [14,15]. Amyloid β protein has been shown to bind metal ions with high affinity, while iron and zinc exposure induces the aggregation and deposition of A β proteins in humans [15,29]. A β plaques have also been associated with MT-I/II in the hippocampus of experimental animal models of AD [21]. Additionally, the activation of astrocytes occurs as a result of A β load, which triggers a secondary astroglial response. An increased number of astrocytes surround A β plaques and, given the capability of astroglia to secrete even minor quantities of amyloid, astroglialosis may contribute alongside neurons to further A β production [30].

Human and animal brain aging has been associated with iron and zinc dyshomeostasis [11,13,14,16,17,26], as well as with MT-I/II expression [31]. The purpose of this study was to investigate the presence and concentration of iron and zinc, in addition to MT-I/II expression, in the brains of aged cats. Through this, an attempt was made to study the correlation between MT-I/II, iron, and zinc with age-related pathological changes, aiming to obtain insights into the mechanisms of a normal aging feline brain. Finally, we prospectively searched for evidence that might further support the hypothesis that cat could be a suitable natural animal model for aging and neurodegeneration.

2. Materials and Methods

2.1. Animals and Allocation into Groups

The study included thirty subjects. The brains from 3 young cats (1 to 2 years old) and 27 aged cats (7 to 20 years old) were obtained. The cats either died by natural causes or traumatic injury or were euthanized in the Companion Animal Clinic (Table 1). No history of neurological signs, mental or behavioral dysfunction was referred upon veterinary examination. Conventional necropsy was performed on all cats.

Table 1. Age, gender, breed, pathological data, and reason for euthanasia or death of the aged cats.

Case No.	Age (Years)	Gender	Breed	Reason for Euthanasia or Death	Case No.	Age (Years)	Gender	Breed	Reason for Euthanasia or Death	
	1	♂	DSH	Gastric and hepatic neoplasia/hypovolemic shock—death	16	>10	♀	DSH	Accident—death	
Controls	2	♂	DSH	Accident—death	17	12	♀	DSH	Septic shock—death	
	3	♀	DSH	Accident—euthanasia	18	12	♀	DSH	Chronic renal and hepatic failure—death	
	4	♂	DSH	Acute leukemia—euthanasia	Senior Group	19	11	♂	Siam	Triaditis—death
	5	♀	Persian	Accident—euthanasia	20	13	♂	DSH	Alimentary lymphoma—death	
	6	7–10	♀	DSH	Accident—death	21	14	♂	DSH	Renal neoplasm—euthanasia
	7	♂	DSH	Chronic renal failure—death	22	>10	♀	DSH	Chronic renal failure—death	
	8	♀	Persian	Arterial thromboembolism—death	23	20	♀	Persian	Polycystic kidney, liver, and pancreas disease—death	
Mature group	9	♂	DSH	Hypertrophic cardiomyopathy—death	24	20	♀	Persian	Chronic renal failure—euthanasia	
	10	♀	DSH	Status epilepticus—pulmonary—death	25	15	♂	DSH	Melanoma—euthanasia	
	11	♀	DSH	Hypovolemic shock—death	Geriatric Group	26	17	♂	DSH	Accident—death
	12	♀	DSH	Lower urinary tract disease—death	27	17	♀	DSH	Chronic renal failure—euthanasia	
	13	♀	DSH	Accident—death	28	16	♀	Persian	Chronic renal and hepatic failure—euthanasia	
	14	♀	DSH	Chronic renal failure—euthanasia	29	15	♀	DSH	Chronic renal failure—death	
	15	♀	Siam	Polycystic kidney disease—euthanasia	30	16	♂	DSH	Peritoneal mesothelioma—death	

Vogt et al., in 2010, mentioned clustering of cats according to their age in the following four groups: Junior (7 months to 2 years old), Mature (7 to 10 years old), Senior (11–14 years old), and Geriatric (≥ 15 years old) [32]. In the present study, the cats were separated as follows: 12 belonged to the Mature group, 7 to the Senior group, and 8 to the Geriatric group. As controls were used the brains of three Junior cats (1.5, 2, and 2 years old).

2.2. Histopathological Examination and Scoring System

Coronal sections were taken from the right cerebral and cerebellar hemisphere. Tissue samples including the frontal and temporal grey (GM) and white (WM) matter, hippocampus, striatum, thalamus, and cerebellum were fixed in 10% neutral-buffered formalin, which was replaced after 2 days of fixation. Subsequently, they were embedded in paraffin wax and cut into 4–6 μm thick sections. Serial sections from each sample were stained with hematoxylin and eosin (H-E), Klüver–Barrera (KB), and Periodic acid–Schiff (PAS).

Histopathological lesions were scored using an optical microscope Nikon eclipse 50i. Lesions such as neuronophagia, satellitosis, chromatolysis, neuron and microglial lipofuscin deposits, neuronal vacuolation, neuronal necrosis and loss, perivascular microglia, neuroaxonal degeneration, white and grey matter vacuolation, cortical vascular fibrosis and hyalinosis, leptomeningeal fibrosis, leptomeningeal vessel (LV) fibrosis, LV and choroid plexus vessel (CPV) hyalinosis, LV calcification, choroid plexus (CP) epithelial and vascular fibrosis, and hemorrhages were scored as follows: **0**, no staining; **1**, detected in <25% of the examined areas; **2**, detected in 25–50% of the examined areas; **3**, detected in >50% of the examined areas. Additionally, the presence of axonal spheroids, Lafora-like bodies, and H-E-positive bodies was scored as follows: **0**, no staining; **1**, <10 bodies; **2**, 10–20 bodies; **3**, >20 bodies.

2.3. Prussian Blue–Diaminobenzidine (DAB)-Enhanced Histochemical Staining (Perl's/DAB) and Scoring System

After deparaffinization and rehydration, sequential sections taken from the above samples were treated with 3,6% hydrogen peroxide for 15 min to block endogenous peroxidase activity. After washing in distilled water for 3–5 min, sections were incubated in a 1:1 freshly prepared mixture of 2% HCl and 2% potassium ferrocyanide at room temperature for 30 min. This protocol is consistent with the standard Perl's reaction and gives blue coloration of the non-heme iron accumulation. Iron signals were additionally enhanced in a 3,3'-diaminobenzidine tetrahydrochloride (DAB) intensification procedure following Meguro's modification [33], as described by Sukhorukova et al., 2013 [34]. Following the standard Perls' reaction, the sections were washed 3 times for 5 min in DW (3 portions for 3–5 min) and then treated with a chromogen, DAB (Dako, Glostrup, Denmark), for 10–12 min. The exact time of treatment was adjusted according to development of optimal staining with DAB in the control preparations knowingly containing Fe³⁺. Finally, preparations were counterstained with 0.5% nuclear fast red (Sigma-Aldrich, Burlington, MA, USA).

Scoring of cytoplasmic neuronal and glial iron was evaluated by counting the number of positively stained cells in 10 consecutive high-power fields (40×). No staining was scored as **0**; a mean number of cells <20 as **1**; 20–30 cells as **2**; and >30 as **3** in the temporal and frontal GM and WM, hippocampus, striatum, thalamus, cerebellar cortex, and dentate nucleus.

In order to assess iron plaque load, we counted the total number of plaques per section. No staining was scored as **0**; PC <20 was scored as **1**; 20–30 as **2**; and >30 as **3** in the frontal and temporal GM and WM, hippocampus, striatum, thalamus, cerebellar GM and WM, and dentate nucleus.

Finally, detection of myelin-associated iron in the cerebral and cerebellar white matter and in the myelin-rich cerebral cortical layers, IV and V, was scored as follows: **0**, no staining; **1**, detected in <25% of the examined areas; **2**, detected in 25–50% of the examined areas; **3**, detected in >50% of the examined areas.

2.4. Immunohistochemistry Using Antibodies against MT-I/II, GFAP, and Aβ42

Immunohistochemistry was performed using a Super Sensitive Polymer-HRP IHC Detection System (BioGenex, Fremont, CA, USA). The primary antibodies used are listed in Table 2. Deparaffinized sections after EDTA microwave incubation (EnvisionFLEX, Target retrieval solution, high pH, Dako, Glostrup, Denmark) for 20–30 min at 500 watts (95–100 °C) for epitope retrieval were then treated with 3.6% hydrogen peroxide (H₂O₂)—methanol at room temperature for 30 min. They were subsequently incubated in 10% NGS at 37 °C for 30 min to avoid nonspecific reactions. The sections were then incubated at 4 °C overnight with one of the primary antibodies. After washing three times in PBS, sections were incubated with poly-HRP reagent (from Super Sensitive Polymer-HRP IHC Detection system) at room temperature for 40 min. Then, sections were washed with PBS and visualized with 0.05% 3-3' diaminobenzidine and 0.03% H₂O₂ in DW. Counterstaining was performed with Delafield hematoxylin. As positive controls for antibodies against

MT-I/II, tissue sections from feline kidney samples were used, and for GFAP and A β 42, sections from previously tested aged feline brain samples were used [6]. As negative controls, sections where the primary antibody was replaced by PBS were used.

Table 2. Antibodies used in the current study.

Antibody	Dilution	Source	Pretreatment
Anti-MT-I/II	1:200	Novus Biologicals	EDTA high pH (EnvisionFLEX, Target retrieval solution, high pH, Dako, Glostrup, Denmark)
Anti-GFAP	1:400	Dako, Denmark	None
Anti-amyloid β 42	1:800	EMD Millipore, USA	Formic acid 87% (AnalaR NORMAPUR)

2.5. Immunohistochemical Evaluation

MT-I/II expression was scored by calculating the mean number of positively stained neurons and astrocytes in 10 consecutive high-power fields (40 \times original magnification). The regions examined involved the grey and white matter of frontal and temporal GM and WM and the GM and WM (alveus and fimbria) of hippocampus, striatum, and thalamus. No staining was scored as 0; a mean number of cells < 12 as 1; 12–24 cells as 2; and >24 as 3.

For MT-I/II scoring in LV, GM and WM, blood vessels of the temporal and frontal lobes, hippocampal, thalamic and striatum blood vessels, frontal leptomeningeal cells (LCs), CPV, and CP epithelial cells, as well as ependymal cells, no staining was scored as 0 and positive staining was scored as 1.

Tissue sections examined immunohistochemically for GFAP were evaluated by performing both morphological and quantitative analysis. Astrocytic GFAP grading based on morphological and quantitative criteria was classified according to Boos et al. (2021), as described in Table 3 [35]. The number of GFAP-positive astrocytes was assessed by calculating the mean number of astrocytes counted in five random fields (20 \times original magnification).

Table 3. Combined evaluation of GFAP-positive astrocytes in the brain of aged cats, using both quantitative and morphological criteria (Boos et al. 2021).

	Grade 0	Grade 1	Grade 2	Grade 3
Quantitative criteria	0–30 cells	16–60 cells	40–100 cells	>77 cells
Morphological alterations	Absence of nucleus alterations and a few mildly stained cells with long, thin, well-ramified cytoplasmic processes	Mildly increased nuclei volume and mildly stained long, thin, well-ramified cytoplasmic processes	Moderately increased nuclei volume and moderately stained long, moderately thickened cytoplasmic processes	Severely increased nuclei volume (gemistocytes) and intensely stained thickened cytoplasmic processes trespassing other cells processes

We immunohistochemically evaluated the presence of A β deposits in the LV wall (cerebral amyloid angiopathy/CAA) and GM and WM CAA, A β accumulation in neurons and astrocyte A β deposition in CPV and CP epithelial cells, and A β plaque load.

For leptomeningeal CAA, we used the following scoring system: 0, no staining; 1, mild (A β deposits were detected in <25% of the vessels); 2, moderate (A β deposits were detected in 25–50% of the vessels); 3, severe (A β deposits were detected >50% of the vessels), in the leptomeninges of the frontal and temporal lobes as well as the cerebellum.

To score CAA (affecting arterioles and capillaries) in GM and WM of the temporal and frontal lobes as well as the cerebellum, areas in which more than 10 A β -positive vessels were detected in 20 \times original magnification were defined as “strongly CAA-affected areas”. CAA was classified as follows: 0, no A β deposition in blood vessels; 1, mild (less than 10 A β -positive blood vessels or only 1 strongly CAA-affected area was seen in the entire GM and WM); 2, moderate (2 to 4 strongly CAA-affected areas were seen in the entire GM and WM); 3, severe (more than 5 strongly CAA-affected areas were seen in the entire GM and WM) (modified by [36]).

A β accumulation in neurons and astrocytes was assessed by counting the total number of positively stained cells in 10 consecutive high-power fields (40 \times). Tissue sections from the temporal and frontal GM and WM, hippocampus, striatum, thalamus, cerebellar GM and WM, and dentate nucleus were evaluated. No staining was scored as 0; a mean number of cells < 10 as 1; 10–20 cells as 2; and >20 as 3.

A β deposition in CPV and CP epithelial cells was evaluated and scored as follows: 0, no staining; 1, mild (A β deposits were detected in <25% of the CPV and CP epithelial cells); 2, moderate (A β deposits were detected in 25–50% of the CPV and CP epithelial cells); 3, severe (A β deposits were detected >50% of the CPV and CP epithelial cells).

Finally, regarding A β plaque load, the total number of senile plaques (SPs) was counted in the frontal and temporal GM and WM, hippocampus, striatum, thalamus, cerebellar grey and white matter, and dentate nucleus. No staining was scored as 0; a PC < 10 was scored as 1; 10–20 as 2; and > 20 as 3.

2.6. Determination of Iron and Zinc in Brain Tissue by Inductively Coupled Plasma Mass Spectrometry (ICP-MS)

2.6.1. Sample Preparation

Since trace amounts of analyte metals are ubiquitous in the environment and may be present in dust particles, care was taken to avoid external contamination during each step of the sample preparation. Efforts were made to use only polypropylene, polystyrene, and stainless-steel labware to minimize elemental backgrounds. Porcelain evaporation capsules were also used in the drying chamber in order to reach higher temperatures. Only powder-free gloves were used. Deionized and ultrapure water (Millipore Milli-Q water purification system) was used throughout the process. All sample storage containers and other equipment used were soaked for at least 24 h in 10% HNO₃ and then rinsed copiously with ultrapure water.

Coronal sections from the left hemisphere of the frontal, parietal, occipital, and temporal lobes, as well as the left cerebellar hemisphere, were collected and then placed as a total in small polypropylene containers. The tissue segments were of the same width per region and were cut using an acid-washed quartz knife on an acid-washed polypropylene board. The sampled, complete tissue mass was mixed with 10 drops of ultrapure water and homogenized using the Ultra-Turrax Model T-25 homogenizer (Jahnke & Kunkel IKA, Staufen, Germany). Samples were dried at 105 °C for 24 h in a drying and heating chamber (Binder, Model ED56). The weight of the brain samples was determined before and after drying for at least 24 h until constant weight was achieved. The dry weight of each sample was 0.5–1.0 g. Three samples (Controls) were prepared as duplicates.

Samples were digested in sealed TFM vessels in a microwave digestion oven (Milestone MLS 1200) after 7 mL of 65% HNO₃ (Merck, Suprapur, Darmstadt, Germany) and 3 mL H₂O₂ 30% w/w (Carlo Herba, Cornaredo, Italy) were added. After acid digestion, no visual solid residual remained. The Teflon vessels were allowed to cool to room temperature. Subsequently, samples were quantitatively recovered by filtration in 50 mL class A volumetric flasks and diluted to 50 mL with HNO₃ 2%.

2.6.2. Instrumentation

An Agilent 7900 ICP-MS automated quadrupole ICP-MS instrument was used for the analysis of brain tissues for iron and zinc. The estimated concentrations of iron and zinc were expressed in $\mu\text{g/g}$.

2.7. Statistical Analysis

Iron and zinc concentrations in the brain of the selected cats were analyzed with one-way ANOVA using SPSS 28.0 (BM SPSS Statistics for Windows, Version 28.0. Armonk, NY, USA: IBM Corp.), while post hoc comparisons between groups were investigated using Duncan's test. Statistical analysis of the scores (H-E, PAS, KB, and Perl's/DAB histochemical staining, as well as A β , GFAP, and MT-I/II immunolabeling) was performed

using chi-squared tests applied with SPSS as well as with the use of GraphPad Prism (version 9.1.2 for Windows[®], GraphPad Software, San Diego, CA, USA). The level of significance was set at $p < 0.05$, and statistically significant trends (#) were underlined for $p \leq 0.1$.

3. Results

Following natural death or euthanasia, a total of 30 cat brains were collected at necropsy, and their ages ranged from 1.5 to 20 years old. Almost a third of the cats were males (36.7%, $n = 11$), whereas two-thirds (63.3%, $n = 19$) were females.

3.1. Histopathological Findings

Age-related lesions were not observed in the Controls. On the other hand, changes such as neuronophagia, satellitosis, chromatolysis, neuron and microglial lipofuscin deposits, neuronal necrosis and loss, perivascular infiltration of macrophages, neuroaxonal degeneration, and white and grey matter vacuolation were seen to a variable degree in the frontal and temporal lobe as well as the cerebellum of aged cats (Table 4, Table S1).

Table 4. Histopathological scoring of age-related brain lesions in mature, senior, and geriatric cats.

Investigated Parameter	Grading Score	Groups				Significance (Chi Square)
		Controls	Mature	Senior	Geriatric	
Neuronophagia	0	100% (3)	0%	0%	0%	$p < 0.001$
	1	0%	91.7% (11)	71.4% (5)	0%	
	2	0%	8.3% (1)	28.6% (2)	50% (4)	
	3	0%	0%	0%	50% (4)	
	Total	100% (3)	100% (12)	100% (7)	100% (8)	
Satellitosis	0	100% (3)	0%	0%	0%	$p < 0.001$
	1	0%	75% (9)	42.9% (3)	0%	
	2	0%	16.7% (2)	57.1% (4)	50% (4)	
	3	0%	8.3% (1)	0%	50% (4)	
	Total	100% (3)	100% (12)	100% (7)	100% (8)	
Chromatolysis	0	100% (3)	0%	0%	0%	$p < 0.001$
	1	0%	66.7% (8)	14.3% (1)	0%	
	2	0%	33.3% (4)	85.7% (6)	50% (4)	
	3	0%	0%	0%	50% (4)	
	Total	100% (3)	100% (12)	100% (7)	100% (8)	
Neuronal lipofuscin deposits	0	100% (3)	0%	0%	0%	$p < 0.001$
	1	0%	41.7% (5)	14.2% (1)	0%	
	2	0%	58.3% (7)	42.9% (3)	12.5% (1)	
	3	0%	0	42.9% (3)	87.5% (7)	
	Total	100% (3)	100% (12)	100% (7)	100% (8)	
Neuronal vacuolation	0	100% (3)	66.7% (8)	85.7% (6)	50% (4)	Non-significant
	1	0%	33.3% (4)	14.3% (1)	25% (2)	
	2	0%	0%	0%	25% (2)	
	3	0%	0%	0%	0%	
	Total	100% (3)	100% (12)	100% (7)	100% (8)	

Table 4. Cont.

Investigated Parameter	Grading Score	Groups				Significance (Chi Square)
		Controls	Mature	Senior	Geriatric	
Neuronal necrosis and loss	0	100% (3)	0%	0%	0%	$p < 0.001$
	1	0%	83.3% (10)	28.6% (2)	0%	
	2	0%	16.7% (2)	71.4% (5)	75% (6)	
	3	0%	0%	0%	25% (2)	
	Total	100% (3)	100% (12)	100% (7)	100% (8)	
Microglial lipofuscin deposits	0	100% (3)	0%	0%	0%	$p < 0.001$
	1	0%	83.3% (10)	14.3% (1)	0%	
	2	0%	16.7% (2)	71.4% (5)	25% (2)	
	3	0%	0	14.3% (1)	75% (6)	
	Total	100% (3)	100% (12)	100% (7)	100% (8)	
Perivascular microglia	0	100% (3)	0%	0%	0%	$p < 0.001$
	1	0%	100% (12)	71.4% (5)	37.5% (3)	
	2	0%	0%	28.6% (2)	37.5% (3)	
	3	0%	0%	0%	25% (2)	
	Total	100% (3)	100% (12)	100% (7)	100% (8)	
Spheroids	0	100% (3)	75% (9)	85.7% (6)	62.5% (5)	Non-significant
	1	0%	16.7% (2)	14.3% (1)	12.5% (1)	
	2	0%	8.3% (1)	0%	25% (2)	
	3	0%	0%	0%	0%	
	Total	100% (3)	100% (12)	100% (7)	100% (8)	
Lafora-like bodies	0	100% (3)	8.3% (1)	0%	0%	$p < 0.001$
	1	0%	66.7% (8)	57.1% (4)	12.5% (1)	
	2	0%	25% (3)	28.6% (2)	62.5% (5)	
	3	0%	0%	14.3% (1)	25% (2)	
	Total	100% (3)	100%	100%	100%	
H-E-positive bodies	0	100% (3)	58.4% (7)	85.7% (6)	0%	$p = 0.014$
	1	0%	33.3% (4)	0%	62.5% (5)	
	2	0%	8.3% (1)	14.3% (1)	37.5% (3)	
	3	0%	0%	0%	0%	
	Total	100% (3)	100% (12)	100% (7)	100% (8)	
Neuroaxonal degeneration	0	100% (3)	0%	0%	0%	$p < 0.001$
	1	0%	83.3% (10)	57.1% (4)	0%	
	2	0%	16.7% (2)	42.9% (3)	25% (2)	
	3	0%	0%	0%	75% (6)	
	Total	100% (3)	100% (12)	100% (7)	100% (8)	

Table 4. Cont.

Investigated Parameter	Grading Score	Groups				Significance (Chi Square)
		Controls	Mature	Senior	Geriatric	
GM and WM vacuolation	0	100% (3)	0%	0%	0%	$p < 0.001$
	1	0%	66.7% (8)	57.1% (4)	12.5% (1)	
	2	0%	25% (3)	42.9% (3)	50% (4)	
	3	0%	8.3% (1)	0%	37.5% (3)	
	Total	100% (3)	100% (12)	100% (7)	100% (8)	
GM and WM vascular hyalinosis	0	100% (3)	83.3% (10)	42.9% (3)	25% (2)	$p = 0.040$
	1	0%	16.7% (2)	57.1% (4)	50% (4)	
	2	0%	0%	0%	25% (2)	
	3	0%	0%	0%	0%	
	Total	100% (3)	100% (12)	100% (7)	100% (8)	
GM and WM vascular fibrosis	0	100% (3)	66.7% (8)	28.6% (2)	25% (2)	$p = 0.055$
	1	0%	33.3% (4)	71.4% (5)	75% (6)	
	2	0%	0%	0%	0%	
	3	0%	0%	0%	0%	
	Total	100% (3)	100% (12)	100% (7)	100% (8)	
Leptomeningeal fibrosis	0	100% (3)	33.3% (4)	0%	0%	$p < 0.001$
	1	0%	58.4% (7)	42.9% (3)	12.5% (1)	
	2	0%	8.3% (1)	57.1% (4)	37.5% (3)	
	3	0%	0%	0%	4	
	Total	100% (3)	100% (12)	100% (7)	100% (8)	
LV fibrosis	0	100% (3)	33.3% (4)	0%	0%	$p < 0.001$
	1	0%	41.7% (5)	14.3% (1)	0%	
	2	0%	25% (3)	85.7% (6)	62.5% (5)	
	3	0%	0%	0%	37.5% (3)	
	Total	100% (3)	100% (12)	100% (7)	100% (8)	
LV hyalinosis	0	100% (3)	100% (12)	85.7% (6)	62.5% (5)	Non-significant
	1	0%	0%	14.3% (1)	12.5% (1)	
	2	0%	0%	0%	25% (2)	
	3	0%	0%	0%	0%	
	Total	100% (3)	100% (12)	100% (7)	100% (8)	
LV calcification	0	100% (3)	75% (9)	71.4% (5)	75% (6)	Non-significant
	1	0%	25% (3)	28.6% (2)	25% (2)	
	2	0%	0%	0%	0%	
	3	0%	0%	0%	0%	
	Total	100% (3)	100% (12)	100% (7)	100% (8)	

Table 4. Cont.

Investigated Parameter	Grading Score	Groups				Significance (Chi Square)
		Controls	Mature	Senior	Geriatric	
CPV and CP epithelial fibrosis	0	100% (3)	25% (3)	0%	0%	$p < 0.001$
	1	0%	66.7% (8)	28.6% (2)	0%	
	2	0%	8.3% (1)	42.8% (3)	37.5% (3)	
	3	0%	0%	28.6% (2)	62.5% (5)	
	Total	100% (3)	100% (12)	100% (7)	100% (8)	
CPV hyalinosis	0	100% (3)	100% (12)	71.4% (5)	62.5% (5)	Non-significant
	1	0%	0%	28.6% (2)	37.5% (3)	
	2	0%	0%	0%	0%	
	3	0%	0%	0%	0%	
	Total	100% (3)	100% (12)	100% (7)	100% (8)	
Hemorrhages	0	100% (3)	75% (9)	100% (7)	62.5% (5)	Non-significant
	1	0%	25% (3)	0%	37.5% (3)	
	2	0%	0%	0%	0%	
	3	0%	0%	0%	0%	
	Total	100% (3)	100% (12)	100% (7)	100% (8)	

Kruskal–Wallis test. Neuronophagia: Controls vs. Mature Group: $p = 0.044$, Controls vs. Senior group: $p = 0.021$, Controls vs. Geriatric group: $p < 0.001$, Mature vs. Geriatric group: $p < 0.001$, Senior vs. Geriatric group: $p = 0.008$; Satellitosis: Controls vs. Mature Group: $p = 0.043$, Controls vs. Senior group: $p = 0.016$, Controls vs. Geriatric group: $p < 0.001$, Mature vs. Geriatric group: $p = 0.003$, Senior vs. Geriatric group: $p = 0.049$; Chromatolysis: Controls vs. Mature Group: $p = 0.063^{\#}$, Controls vs. Senior group: $p = 0.005$, Controls vs. Geriatric group: $p < 0.001$, Mature vs. Geriatric group: $p = 0.001$; Neuronal lipofuscin deposits: Controls vs. Mature Group: $p = 0.080^{\#}$, Controls vs. Senior group: $p = 0.005$, Controls vs. Geriatric group: $p < 0.001$, Mature vs. Senior group: $p = 0.087^{\#}$, Mature vs. Geriatric group: $p < 0.001$; Neuronal necrosis and loss: Controls vs. Mature Group: $p = 0.068^{\#}$, Controls vs. Senior group: $p = 0.003$, Controls vs. Geriatric group: $p < 0.001$, Mature vs. Senior group: $p = 0.077^{\#}$, Mature vs. Geriatric group: $p < 0.001$; Microglial lipofuscin deposits: Controls vs. Senior group: $p = 0.004$, Controls vs. Geriatric group: $p < 0.001$, Mature vs. Senior group: $p = 0.044$, Mature vs. Geriatric group: $p < 0.001$; Perivascular microglia: Controls vs. Mature Group: $p = 0.015$, Controls vs. Senior group: $p = 0.003$, Controls vs. Geriatric group: $p < 0.001$, Mature vs. Geriatric group: $p = 0.010$; Lafora-like bodies: Controls vs. Mature Group: $p = 0.045$, Controls vs. Senior group: $p = 0.012$, Controls vs. Geriatric group: $p < 0.001$, Mature vs. Geriatric group: $p = 0.012$; H-E-positive bodies: Controls vs. Geriatric group: $p = 0.005$, Mature vs. Geriatric group: $p = 0.010$, Senior vs. Geriatric group: $p = 0.003$; Neuroaxonal degeneration: Controls vs. Mature Group: $p = 0.054^{\#}$, Controls vs. Senior group: $p = 0.022$, Controls vs. Geriatric group: $p < 0.001$, Mature vs. Geriatric group: $p < 0.001$, Senior vs. Geriatric group: $p = 0.011$; GM and WM vacuolation: Controls vs. Mature Group: $p = 0.020$, Controls vs. Senior group: $p = 0.023$, Controls vs. Geriatric group: $p < 0.001$, Mature vs. Geriatric group: $p = 0.028$, Senior vs. Geriatric group: $p = 0.069^{\#}$; GM and WM vascular hyalinosis: Controls vs. Geriatric group: $p = 0.020$, Mature vs. Geriatric group: $p = 0.005$; Leptomeningeal fibrosis: Controls vs. Senior group: $p = 0.013$, Controls vs. Geriatric group: $p < 0.001$, Mature vs. Senior group: $p = 0.057^{\#}$, Mature vs. Geriatric group: $p < 0.001$; LV fibrosis: Controls vs. Senior group: $p = 0.008$, Controls vs. Geriatric group: $p < 0.001$, Mature vs. Senior group: $p = 0.036$, Mature vs. Geriatric group: $p < 0.001$; CPV and CP epithelial fibrosis: Controls vs. Senior group: $p = 0.006$, Controls vs. Geriatric group: $p < 0.001$, Mature vs. Senior group: $p = 0.020$, Mature vs. Geriatric group: $p < 0.001$.

Neuronophagia and satellitosis were distributed in layers II–VI in the cerebral cortices, primarily in the frontal lobe, the pyramidal layer of Cornu Ammonis (CA) of the hippocampus, the Purkinje cell layer, and the dentate nuclei. A constant lesion observed in all elderly cats was chromatolysis, particularly in Betz cells, the pyramidal cell layer of the hippocampus, and the Purkinje cell layer. High severity of neuronal loss was noticed in cats aged 20 years old. Complete Purkinje cell loss in some regions was observed in 13 cats over 10 years old (case Nos 4, 16, 17, 19, 20, 21, 23, 24, and 26–30). Additionally, in five of these cases, there was also a reduction in granule cell density (case Nos 20, 23, 24, 27, and 29). Neuronal vacuolation was noticed in 9 of the 27 aged cats. Single or multiple variable

size intracytoplasmic vacuoles were primarily found in the neurons of the cerebral cortices as well as in Purkinje and Golgi type II neurons.

Regarding vascular lesions, medial hyalinosis and adventitial fibrosis of small arteries and arterioles were found in the GM and WM, meninges, and CP. Additionally, calcification of the LV wall was noted in seven aged cats over 8 years old. Leptomeningeal thickening due to an increase in collagen fibers was observed in almost all brains (25/27 cases).

Three types of bodies were observed. Lafora-like bodies detected in the aged brains were more numerous in the cerebellum than in the temporal and frontal lobes. They were distributed within all cortical and cerebellar layers and white matter as well as the dentate nucleus, and they were more prominent in the grey than the white matter. Spheroids were displayed both in grey and white matter in five cases (case Nos 6, 16, 24, 29, and 30). In the cerebellum, they were found in the white matter in three cases (case Nos 4, 11, and 24) and in the granular cell layer in one case (case No 26). H-E-positive bodies were noticed in 14 cats over 8 years old. These homogeneous, round-to-ovoid, non-membrane-bound basophilic bodies were distributed in the neuropil in layers I-II of the cerebral cortices, in the cerebellar molecular layer, and dentate nuclei. The above formations were not associated with reactive lesions in the adjacent neuropil. A few aged animals (six cases) had small foci of hemorrhages (case Nos 9, 11, 12, 24, 26, and 30).

3.2. *Perl's/DAB Scoring*

Perl's/DAB-stained iron deposits were observed within neurons, glial cells, and their cytoplasmic projections in the grey and white matter of the temporal lobe in 25/30 cats. Similar deposits were found in the hippocampus (29/30), thalamus (25/30), striatum (15/30), frontal lobe (26/30), and cerebellum (29/30). Positively stained cells were noticed in all cerebral cortical layers (I–VI). The hippocampus revealed positive neuronal staining, most pronounced in the pyramidal cell layer of the CA and dentate gyrus. In the cerebellum, Purkinje cells were primarily stained, but a small number of basket and Golgi type II cells were also positive. Perl's/DAB staining was predominantly detected within the nucleoli, while nuclear and perikarial staining of varying degrees was also observed.

Perl's/DAB histochemical staining revealed the presence of extracellular deposits in the gray and white matter forming two types of iron plaques (IPs) that shared morphological similarities with Abeta-positive senile plaques. Thus, since the first type was characterized by focal spherical deposits with a dense core, it was named "condensed iron plaque". The second type was characterized by large, diffuse, and poorly delimited deposits and was named "diffuse iron plaque" (Figure S1). Condensed IPs were the predominant type, and both types were detected in all examined brain regions. Plaque staining in the cortex was present in all cortical layers. In animals with scanty deposits, the plaques were distributed in IV/V cortical layers. The IPs were noticed in greater numbers in grey matter compared to white matter. In the hippocampus, IPs were principally noticed in the CA2, CA3 subfields, stratum oriens, and stratum lacunosum-moleculare of the CA, as well as the dentate hilus. In the cerebellum, the abundance of IPs was present in the molecular layer. Plaque formation was also noticed in the striatum and thalamus (Figure 1).

In addition to IPs, band-like iron deposition was found in the white matter of the frontal and temporal lobes and the cerebellum, representing myelin-associated iron. Band-like depositions were also noticed in the thalamus in 4/30 cats (9 years old) and in the fimbria of the hippocampus in 3/30 aged cats (>12 years old) (Table 5, Table S2).

Table 5. Iron deposition scoring in the brains of aged cats.

Investigated Parameter	Grading Score	Groups				Significance (Chi Square)
		Controls	Mature	Senior	Geriatric	
Temporal GM and WM cells	0	0%	33.3% (4)	0%	12.5% (1)	Non-significant
	1	66.7% (2)	41.7% (5)	85.7% (6)	25% (2)	
	2	33.3% (1)	16.7% (2)	0%	75% (6)	
	3	0%	8.3% (1)	14.3% (1)	25% (2)	
	Total	100% (3)	100% (12)	100% (7)	100% (8)	
Temporal GM and WM IPs	0	0%	0%	0%	0%	Non-significant
	1	66.7% (2)	50% (6)	42.8% (3)	12.5% (1)	
	2	33.3% (1)	41.7% (5)	28.6% (2)	37.5% (3)	
	3	0%	8.3% (1)	28.6% (2)	50% (4)	
	Total	100% (3)	100% (12)	100% (7)	100% (8)	
Temporal WM MF *	0	100% (3)	50% (6)	42.8% (3)	25% (2)	Non-significant
	1	0%	41.7% (5)	14.3% (1)	37.5% (3)	
	2	0%	0%	14.3% (1)	12.5% (1)	
	3	0%	8.3% (1)	28.6% (2)	25% (2)	
	Total	100% (3)	100% (12)	100% (7)	100% (8)	
Hippocampal cells	0	0%	8.3% (1)	0%	0%	Non-significant
	1	66.7% (2)	66.7% (8)	71.4% (5)	37.5% (3)	
	2	0%	0%	14.3% (1)	37.5% (3)	
	3	33.3% (1)	25% (3)	14.3% (1)	25% (2)	
	Total	100% (3)	100% (12)	100% (7)	100% (8)	
Hippocampal IPs	0	66.7% (2)	16.7% (2)	14.3% (1)	0%	Non-significant
	1	33.3% (1)	75% (9)	57.1% (4)	75% (6)	
	2	0%	8.3% (1)	28.6% (2)	12.5% (1)	
	3	0%	0%	0%	12.5% (1)	
	Total	100% (3)	100% (12)	100% (7)	100% (8)	
Thalamic cells	0	0%	33.3% (4)	14.3% (1)	0%	Non-significant
	1	100% (3)	66.7% (8)	85.7% (6)	75% (6)	
	2	0%	0%	0%	12.5% (1)	
	3	0%	0%	0%	12.5% (1)	
	Total	100% (3)	100% (12)	100% (7)	100% (8)	
Thalamic IPs	0	100% (3)	0%	0%	0%	$p = 0.025$
	1	0%	66.7% (8)	57.1% (4)	12.5% (1)	
	2	0%	33.3% (4)	14.3% (1)	25% (2)	
	3	0%	0%	28.6% (2)	62.5% (5)	
	Total	100% (3)	100% (12)	100% (7)	100% (8)	
Striatal cells	0	100% (3)	50% (6)	42.9% (3)	37.5% (3)	Non-significant
	1	0%	41.7% (5)	57.1% (4)	50% (4)	
	2	0%	8.3% (1)	0%	12.5% (1)	
	3	0%	0%	0%	0%	
	Total	100% (3)	100% (12)	100% (7)	100% (8)	

Table 5. Cont.

Investigated Parameter	Groups					Significance (Chi Square)
	Grading Score	Controls	Mature	Senior	Geriatric	
Striatal IPs	0	33.3% (1)	16.7% (2)	28.6% (2)	12.5% (1)	Non-significant
	1	66.7%(2)	83.3% (10)	71.4% (5)	75% (6)	
	2	0%	0%	0%	12.5% (1)	
	3	0%	0%	0%	0%	
	Total	100% (3)	100% (12)	100% (7)	100% (8)	
Frontal GM and WM cells	0	33.3% (1)	16.7% (2)	14.3% (1)	0%	Non-significant
	1	66.7%(2)	66.7% (8)	71.4% (5)	62.5% (5)	
	2	0%	8.3% (1)	14.3% (1)	37.5% (3)	
	3	0%	8.3% (1)	0%	0%	
	Total	100% (3)	100% (12)	100% (7)	100% (8)	
Frontal GM and WM IPs	0	0%	16.7% (2)	0%	0%	$p = 0.088$ #
	1	100% (3)	58.4% (7)	57.1% (4)	12.5% (1)	
	2	0%	16.7% (2)	42.9% (3)	50% (4)	
	3	0%	8.3% (1)	0%	37.5% (3)	
	Total	100% (3)	100% (12)	100% (7)	100% (8)	
Frontal WM MF *	0	100% (3)	41.7% (5)	42.9% (3)	12.5% (1)	Non-significant
	1	0%	41.7% (5)	42.9% (3)	25% (2)	
	2	0%	16.6% (2)	14.2% (1)	37.5% (3)	
	3	0%	0%	0%	25% (2)	
	Total	100% (3)	100% (12)	100% (7)	100% (8)	
Cerebellar GM, WM, and DN * cells	0	0%	0%	14.3% (1)	0%	Non-significant
	1	100% (3)	66.7% (8)	28.6% (2)	37.5% (3)	
	2	0%	25% (3)	57.1% (4)	37.5% (3)	
	3	0%	8.3% (1)	0%	25% (2)	
	Total	100% (3)	100% (12)	100% (7)	100% (8)	
Cerebellar GM, WM, and DN * IPs	0	33.3% (1)	0%	0%	0%	Non-significant
	1	33.3% (1)	58.3% (7)	14.2% (1)	37.5% (3)	
	2	33.4% (1)	25% (3)	42.9% (3)	25% (2)	
	3	0%	16.7% (2)	42.9% (3)	37.5% (3)	
	Total	100% (3)	100% (12)	100% (7)	100% (8)	
Cerebellar WM MF *	0	66.7% (2)	25% (3)	14.3% (1)	0%	$p = 0.002$
	1	33.3% (1)	50% (6)	57.1% (4)	0%	
	2	0%	25% (3)	14.3% (1)	12.5% (1)	
	3	0%	0%	14.3% (1)	87.5% (7)	
	Total	100% (3)	100% (12)	100% (7)	100% (8)	

Kruskal–Wallis test. Thalamic IPs: Controls vs. Geriatric group: $p = 0.008$, Mature vs. Geriatric group: $p = 0.004$, Senior vs. Geriatric group: $p = 0.069$ #; Frontal GM and WM IPs: Controls vs. Geriatric group: $p = 0.018$, Mature vs. Geriatric group: $p = 0.003$, Senior vs. Geriatric group: $p = 0.063$; Frontal WM MF: Controls vs. Geriatric group: $p = 0.005$, Mature vs. Geriatric group: $p = 0.038$, Senior vs. Geriatric group: $p = 0.057$; Cerebellar WM MF: Controls vs. Geriatric group: $p < 0.001$, Mature vs. Geriatric group: $p < 0.001$, Senior vs. Geriatric group: $p = 0.007$. * MF: myelinated fibers; DN: dentate nucleus.

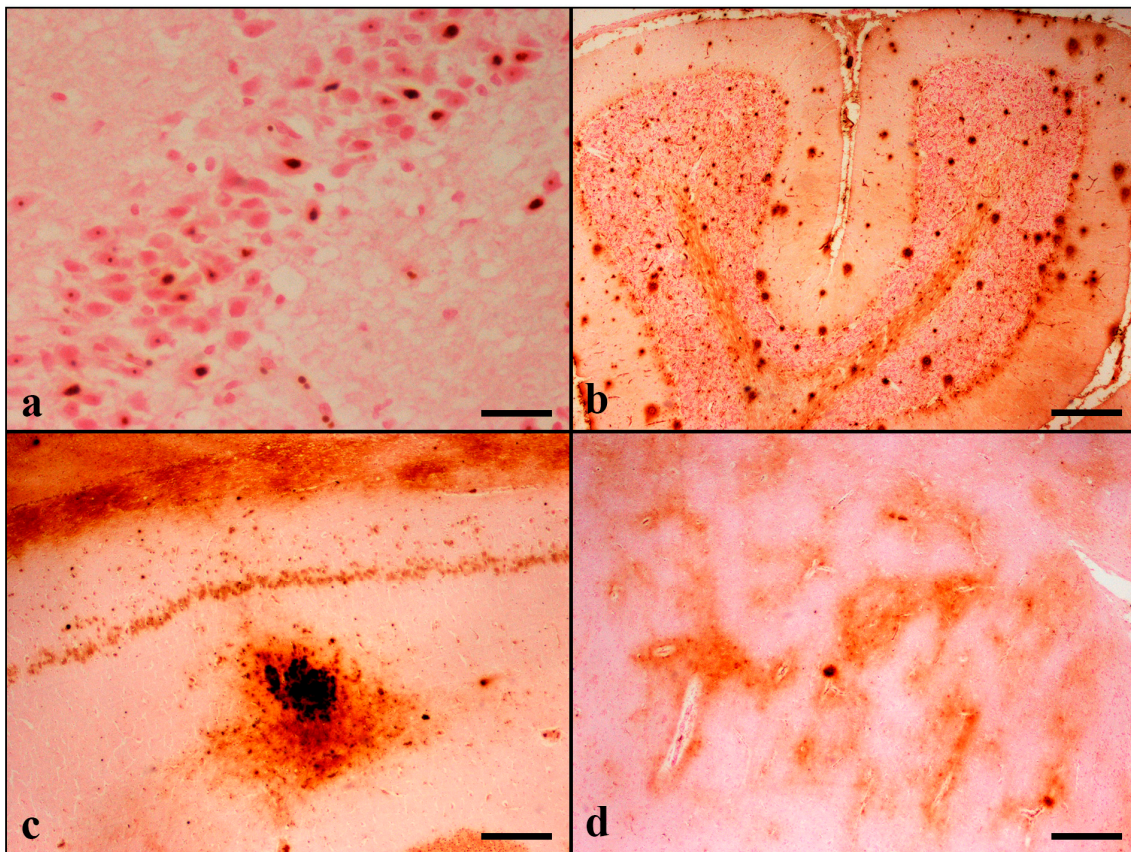


Figure 1. (a) Intense nuclear and nucleolar staining of neurons of the dentate gyrus (case no 5). (b) Condensed and diffuse IPS in all cerebellar layers of the cerebellar cortex and in the white matter. Purkinje, Golgi type II, basket, and glial cells are stained (case no 9). (c) Numerous coalescing condensed iron plaques throughout the hippocampal stratum lacunosum-moleculare and stratum radiatum. Neurons, glial cells, and axons around the coalescing plaques are also stained. CA1 pyramidal cell layer shows cytoplasmic staining. Notice the diffuse band-like iron deposits in the hippocampal alveus indicating myelin-associated iron (case No 27). (d) Multiple Perl's/DAB-positive areas representing myelinated fibers as well as positive glial cells in the thalamus. Two condensed iron plaques are also displayed (case No 6). Perl's/Dab. (a) Bar = 25 μm , (b–d) Bar = 250 μm .

3.3. Immunohistochemical Results

MT-I/II immunoreactive cells were detected in the grey and white matter of the temporal and frontal lobes, hippocampus, thalamus, and striatum, as well as the internal capsule of all 30 animals. They were seen throughout cerebral cortical layers II to V. In the hippocampus, the highest MT-I/II immunolabeling was detected in the CA4 and CA3 subfields, stratum oriens, and stratum lacunosum-moleculare of CA, as well as the dentate molecular layer and hilus. The presence of MT-I/II-positive astrocytes was a constant finding in all cat brains examined, contrarily to neurons, which were occasionally positively stained. A small number of immunoreactive neurons was noticed only in 1 aged cat in the temporal cortex (case No 28), whereas positive staining of the frontal cortex was observed in 14 cases (case Nos 4–6, 9, 11, 14, 16–18, 23–26, and 28). Noteworthy, the Controls did not display neuronal immunoreactivity. Detailed results are summarized in Tables 6 and S3.

Table 6. Scoring of MT-I/II immunolabeling in cats of different ages.

Investigated Parameter	Grading Score	Groups				Significance (Chi Square)
		Controls	Mature	Senior	Geriatric	
Temporal GM	0	33.3% (1)	0%	0%	0%	$p < 0.001$
	1	66.7% (2)	100% (12)	71.4% (5)	12.5% (1)	
	2	0%	0%	28.6% (2)	50% (4)	
	3	0%	0%	0%	37.5% (3)	
	Total	100% (3)	100% (12)	100% (7)	100% (8)	
Temporal WM	0	33.3% (1)	0%	0%	0%	$p < 0.001$
	1	66.7% (2)	91.7% (11)	14.3% (1)	0%	
	2	0%	8.3% (1)	71.4% (5)	25% (2)	
	3	0%	0%	14.3% (1)	75% (6)	
	Total	100% (3)	100% (12)	100% (7)	100% (8)	
Temporal LV	0	0%	16.7% (2)	0%	0%	Non-significant
	1	100% (3)	83.3% (10)	100% (7)	100% (8)	
	2	0%	0%	0%	0%	
	3	0%	0%	0%	0%	
	Total	100% (3)	100% (12)	100% (7)	100% (8)	
Temporal GM and WM vessels	0	0%	25% (3)	0%	12.5% (1)	Non-significant
	1	100% (3)	75% (6) (9)	100% (7)	87.5% (7)	
	2	0%	0%	0%	0%	
	3	0%	0%	0%	0%	
	Total	100% (3)	100% (12)	100% (7)	100% (8)	
Hippocampal GM	0	33.3% (1)	0%	0%	0%	$p = 0.001$
	1	33.3% (1)	16.7% (2)	14.3% (1)	0%	
	2	33.3% (1)	83.3% (10)	71.4% (5)	25% (2)	
	3	0%	0%	14.3% (1)	75% (6)	
	Total	100% (3)	100% (12)	100% (7)	100% (8)	
Hippocampal WM	0	33.3% (1)	0%	0%	0%	$p = 0.041$
	1	33.3% (1)	16.7% (2)	14.3% (1)	0%	
	2	33.3% (1)	83.3% (10)	71.4% (5)	62.5% (5)	
	3	0%	0%	14.3% (1)	37.5% (3)	
	Total	100% (3)	100% (12)	100% (7)	100% (8)	
Hippocampal vessels	0	100% (3)	83.3% (10)	57.1% (4)	25% (2)	$p = 0.030$
	1	0%	16.7% (2)	42.9% (3)	75% (6)	
	2	0%	0%	0%	0%	
	3	0%	0%	0%	0%	
	Total	100% (3)	100% (12)	100% (7)	100% (8)	

Table 6. Cont.

Investigated Parameter	Grading Score	Groups				Significance (Chi Square)
		Controls	Mature	Senior	Geriatric	
Thalamus	0	33.3% (1)	0%	0%	0%	$p < 0.001$
	1	33.3% (1)	75% (9)	42.9% (3)	0%	
	2	33.3% (1)	25% (3)	57.1% (4)	25% (2)	
	3	0%	0%	0%	75% (6)	
	Total	100% (3)	100% (12)	100% (7)	100% (8)	
Thalamic vessels	0	33.3% (1)	83.3% (10)	28.6% (2)	25% (2)	$p = 0.030$
	1	66.7% (2)	16.7% (2)	71.4% (5)	75% (6)	
	2	0%	0%	0%	0%	
	3	0%	0%	0%	0%	
	Total	100% (3)	100% (12)	100% (7)	100% (8)	
Striatum	0	66.7% (2)	8.3%	0%	0%	$p < 0.001$
	1	33.3% (1)	91.7%	85.7% (6)	25% (2)	
	2	0%	0%	14.3% (1)	75% (6)	
	3	0%	0%	0%	0%	
	Total	100% (3)	100% (12)	100% (7)	100% (8)	
Striatal vessels	0	66.7% (2)	83.3% (10)	28.6% (2)	25% (2)	$p = 0.031$
	1	33.3% (1)	16.7% (2)	71.4% (5)	75% (6)	
	2	0%	0%	0%	0%	
	3	0%	0%	0%	0%	
	Total	100% (3)	100% (12)	100% (7)	100% (8)	
Internal capsule	0	0%	0%	0%	0%	$p = 0.017$
	1	66.7% (2)	66.7% (8)	28.6% (2)	0%	
	2	33.3% (1)	33.3% (4)	71.4% (5)	100% (8)	
	3	0%	0%	0%	0%	
	Total	100% (3)	100% (12)	100% (7)	100% (8)	
Frontal GM	0	0%	0%	0%	0%	$p = 0.060^{\#}$
	1	66.7% (2)	58.3% (7)	42.8% (3)	0%	
	2	33.3% (1)	41.7% (5)	28.6% (2)	50% (4)	
	3	0%	0%	28.6% (2)	50% (4)	
	Total	100% (3)	100% (12)	100% (7)	100% (8)	
Frontal WM	0	0%	0%	0%	0%	$p = 0.005$
	1	66.7% (2)	50% (6)	0%	0%	
	2	33.3% (1)	41.7% (5)	71.4% (5)	25% (2)	
	3	0%	8.3% (1)	28.6% (2)	75% (6)	
	Total	100% (3)	100% (12)	100% (7)	100% (8)	

Table 6. Cont.

Investigated Parameter	Grading Score	Groups				Significance (Chi Square)
		Controls	Mature	Senior	Geriatric	
Frontal LC	0	100% (3)	83.3% (10)	71.4% (5)	12.5% (1)	$p = 0.005$
	1	0%	16.7% (2)	28.6% (2)	87.5% (7)	
	2	0%	0%	0%	0%	
	3	0%	0%	0%	0%	
	Total	100% (3)	100% (12)	100% (7)	100% (8)	
Frontal LV	0	0%	8.3% (1)	0%	0%	Non-significant
	1	100% (3)	91.7% (11)	100% (7)	100% (8)	
	2	0%	0%	0%	0%	
	3	0%	0%	0%	0%	
	Total	100% (3)	100% (12)	100% (7)	100% (8)	
Frontal GM and WM vessels	0	66.7% (2)	83.3% (10)	57.1% (4)	50% (4)	Non-significant
	1	33.3% (1)	16.7% (2)	42.9% (3)	50% (4)	
	2	0%	0%	0%	0%	
	3	0%	0%	0%	0%	
	Total	100% (3)	100% (12)	100% (7)	100% (8)	
CP	0	66.7% (2)	66.7% (8)	0%	0%	$p = 0.002$
	1	33.3% (1)	33.3% (4)	100% (7)	100% (8)	
	2	0%	0%	0%	0%	
	3	0%	0%	0%	0%	
	Total	100% (3)	100% (12)	100% (7)	100% (8)	
CPV	0	0%	41.7% (5)	0%	0%	$p = 0.029$
	1	100% (3)	58.3% (7)	100% (7)	100% (8)	
	2	0%	0%	0%	0%	
	3	0%	0%	0%	0%	
	Total	100% (3)	100% (12)	100% (7)	100% (8)	
Ependyma	0	33.3% (1)	16.7% (2)	0%	0%	Non-significant
	1	66.7% (2)	83.3% (10)	100% (7)	100% (8)	
	2	0%	0%	0%	0%	
	3	0%	0%	0%	0%	
	Total	100% (3)	100% (12)	100% (7)	100% (8)	

Kruskal–Wallis test. Temporal GM: Controls vs. Geriatric group: $p < 0.001$, Mature vs. Geriatric group: $p < 0.001$, Senior vs. Geriatric group $p = 0.014$; Temporal WM: Controls vs. Geriatric group: $p < 0.001$, Mature vs. Geriatric group: $p < 0.001$, Controls vs. Senior group: $p = 0.022$, Mature vs. Senior group $p = 0.014$; Hippocampal GM: Controls vs. Geriatric group: $p < 0.001$, Mature vs. Geriatric group: $p = 0.001$, Senior vs. Geriatric group: $p = 0.022$; Hippocampal WM: Controls vs. Geriatric group: $p = 0.004$, group 2 vs. group 4 $p = 0.037$, Controls vs. Senior group: $p = 0.062$ #; Thalamus: Controls vs. Geriatric group: $p = 0.004$, Mature vs. Geriatric group: $p < 0.001$, Senior vs. Geriatric group: $p = 0.010$; STR: Controls vs. Geriatric group: $p < 0.001$, Mature vs. Geriatric group: $p < 0.001$, Controls vs. Senior group: $p = 0.057$, Senior vs. Geriatric group: $p = 0.030$; IC: Controls vs. Geriatric group: $p = 0.048$, Mature vs. Geriatric group: $p = 0.003$.

MT-I/II immunoreactivity was shown in both the nucleus and cytoplasm of astrocytes and in the cytoplasm of neurons and was more intense in cats with severe age-related histopathological changes. A small number of MT-I/II immunoreactive astrocytes was observed in the brain of the control cats. Animals' brains showed positive reactions in

the leptomeningeal, CP, and ependymal cells; LV and blood vessels in GM and WM of both lobes; hippocampal, thalamic, striatal, and CPV regions. Immunoreactive LCs were detected only in the frontal lobe in 11 out of 30 cats, involving only elderly animals. CP epithelial cell immunolabeling was detected in 20 out of 30 cats. MT-I/II immunopositive astrocytes were occasionally observed around blood vessels in cerebral GM and WM (Figure 2).

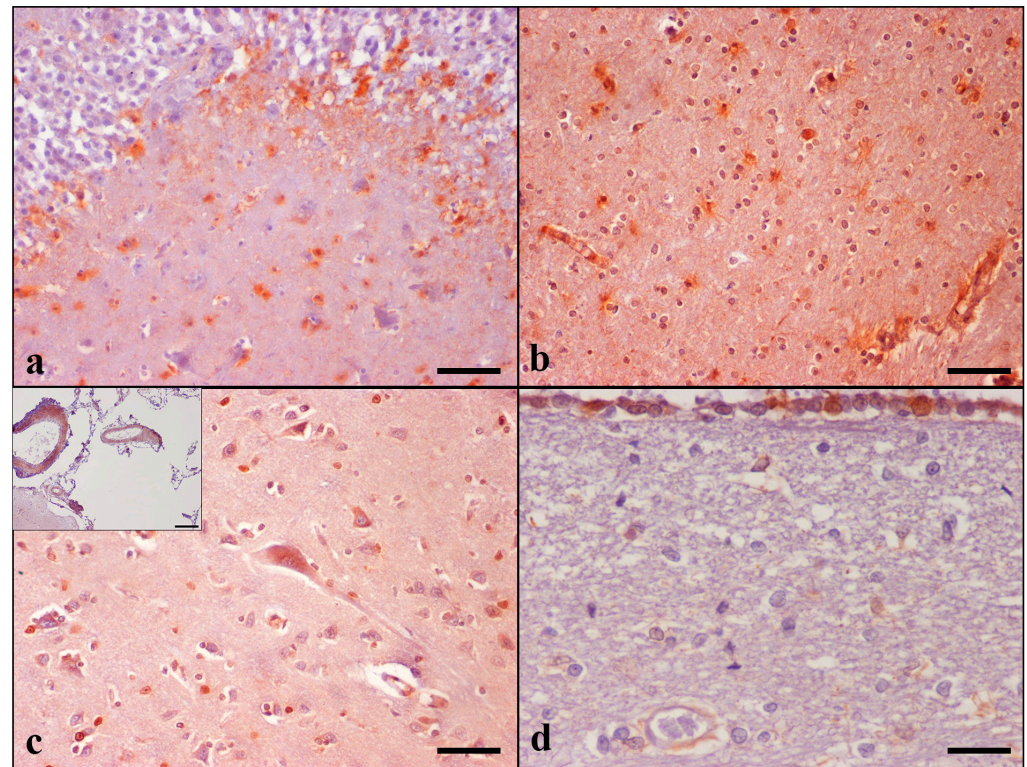


Figure 2. MT-I/II immunolabeling. (a) Positive MT-I/II immunostaining of astrocytes in the DG hilus and CA4 region of the hippocampus (case No 26) and (b) in the temporal cortex. Immunoreactive astrocytes around blood vessels (lower right) (case No 30). (c) Immunolabeling is also occasionally present in the neuronal cytoplasm of the temporal cortex (case No 28). **Inset:** intense immunostaining of the tunica media of the temporal LMV (Case No 24). (d) Ependymal cells showing positive MT-I/II staining in both cytoplasm and nuclei. Positively stained astrocytes are also displayed. IHC, DAB chromogen, hematoxylin counterstain. (a–c) Bar = 50 μ m, ((c) inset) Bar = 100 μ m, (d) Bar = 25 μ m.

Frontal GM: Controls vs. Geriatric group: $p = 0.024$, Mature vs. Geriatric group: $p = 0.002$, Senior vs. Geriatric group $p = 0.095$; Frontal WM: Controls vs. Geriatric group: $p = 0.006$, Mature vs. Senior group: $p = 0.056$ #, Mature vs. Geriatric group: $p < 0.001$; Frontal meningeal cells: Controls vs. Geriatric group: $p = 0.008$, Mature vs. Geriatric group: $p = 0.002$, Senior vs. Geriatric group: $p = 0.020$; CP: Controls vs. Geriatric group: $p = 0.040$, Controls vs. Senior group: $p = 0.044$, Mature vs. Senior group: $p = 0.003$, Mature vs. Geriatric group: $p = 0.002$; CPV: Mature vs. Controls: $p = 0.089$ #, Mature vs. Senior Group: $p = 0.021$, Mature vs. Geriatric Group: $p = 0.016$; Hippocampal vessels: Controls vs. Geriatric group: $p = 0.024$, Mature vs. Geriatric group: $p = 0.009$; Thalamic vessels: Mature vs. Senior Group: $p = 0.024$, Mature vs. Geriatric Group: $p = 0.012$; Striatal vessels: Mature vs. Senior Group: $p = 0.023$, Mature vs. Geriatric Group: $p = 0.012$.

GFAP immunostaining showed diffuse astrogliosis in the frontal and temporal lobes, glia limitans, hippocampus, and cerebellum. Detailed results are summarized in Tables 7 and S4. In the control cats, there were a few GFAP immunoreactive astrocytes with long and thin processes, while the nucleus remained unstained. Astrocytes were

labeled dark brown with the anti-GFAP primary antibody and were generally distributed throughout all cortical layers (Figure 3).

Table 7. Grading of GFAP immunolabeling.

Investigated Parameter	Grading Score	Groups				Significance (Chi Square)
		Controls	Mature	Senior	Geriatric	
Temporal GM	0	100% (3)	0%	0%	0%	$p < 0.001$
	1	0%	16.7% (2)	0%	0%	
	2	0%	75% (9)	42.9% (3)	12.5% (1)	
	3	0%	8.3% (1)	57.1% (4)	87.5% (7)	
	Total	100% (3)	100% (12)	100% (7)	100% (8)	
Temporal WM	0	100% (3)	0%	0%	0%	$p < 0.001$
	1	0%	8.3% (1)	0%	0%	
	2	0%	91.7% (11)	28.6% (2)	0%	
	3	0%	0%	71.4% (5)	100%	
	Total	100% (3)	100% (12)	100% (7)	100% (8)	
Temporal GL	0	100% (3)	0%	0%	0%	$p < 0.001$
	1	0%	58.3% (7)	0%	0%	
	2	0%	41.7% (5)	85.7% (6)	50% (4)	
	3	0%	0%	14.3% (1)	50% (4)	
	Total	100% (3)	100% (12)	100% (7)	100% (8)	
Hippocampal GM	0	100% (3)	0%	0%	0%	$p < 0.001$
	1	0%	16.7% (2)	14.2% (1)	0%	
	2	0%	75% (9)	42.9% (3)	12.5% (1)	
	3	0%	8.3% (1)	42.9% (3)	87.5% (7)	
	Total	100% (3)	100% (12)	100% (7)	100% (8)	
Hippocampal WM	0	100% (3)	0%	0%	0%	$p < 0.001$
	1	0%	16.7% (2)	0%	0%	
	2	0%	83.3% (10)	85.7% (6)	37.5% (3)	
	3	0%	0%	14.3% (1)	62.5% (5)	
	Total	100% (3)	100% (12)	100% (7)	100% (8)	
Hippocampal GL	0	100% (3)	100%	0%	100%	$p < 0.001$
	1	0%	66.7% (8)	0%	0%	
	2	0%	33.3% (4)	100% (7)	62.5% (5)	
	3	0%	0%	0%	37.5% (3)	
	Total	100% (3)	100% (12)	100% (7)	100% (8)	
Frontal GM	0	100% (3)	0%	0%	0%	$p < 0.001$
	1	0%	58.3% (7)	0%	0%	
	2	0%	41.7% (5)	85.7% (6)	37.5% (3)	
	3	0%	0%	14.3% (1)	62.5% (5)	
	Total	100% (3)	100% (12)	100% (7)	100% (8)	

Table 7. Cont.

Investigated Parameter	Grading Score	Groups				Significance (Chi Square)
		Controls	Mature	Senior	Geriatric	
Frontal WM	0	100% (3)	0%	0%	0%	$p < 0.001$
	1	0%	16.7% (2)	0%	0%	
	2	0%	75% (9)	71.4% (5)	25% (2)	
	3	0%	8.3% (1)	28.6% (2)	75% (6)	
	Total	100% (3)	100% (12)	100% (7)	100% (8)	
Frontal GL	0	100% (3)	0%	0%	0%	$p < 0.001$
	1	0%	50% (6)	28.6% (2)	0%	
	2	0%	50% (6)	71.4% (5)	50% (4)	
	3	0%	0%	0%	50% (4)	
	Total	100% (3)	100% (12)	100% (7)	100% (8)	
Cerebellar GM	0	100% (3)	0%	0%	0%	$p < 0.001$
	1	0%	16.7% (2)	0%	0%	
	2	0%	75% (9)	57.1% (4)	12.5% (1)	
	3	0%	8.3% (1)	42.9% (3)	87.5% (7)	
	Total	100% (3)	100% (12)	100% (7)	100% (8)	
Cerebellar WM	0	100% (3)	0%	0%	0%	$p < 0.001$
	1	0%	8.3% (1)	0%	0%	
	2	0%	91.7% (11)	85.7% (6)	12.5% (1)	
	3	0%	0%	14.3% (1)	87.5% (7)	
	Total	100% (3)	100% (12)	100% (7)	100% (8)	
Cerebellar GL	0	100% (3)	0%	0%	0%	$p < 0.001$
	1	0%	66.7% (8)	0%	0%	
	2	0%	33.3% (4)	85.7% (6)	37.5% (3)	
	3	0%	0%	14.3% (1)	62.5% (5)	
	Total	100% (3)	100% (12)	100% (7)	100% (8)	

Kruskal–Wallis test. Temporal GM: Controls vs. Mature Group: $p = 0.062^{\#}$, Controls vs. Senior group: $p = 0.002$, Controls vs. Geriatric group: $p < 0.001$, Mature vs. Senior group: $p = 0.057^{\#}$, Mature vs. Geriatric group: $p = 0.003$; Temporal WM: Controls vs. Senior group: $p = 0.001$, Controls vs. Geriatric group: $p < 0.001$, Mature vs. Senior group: $p = 0.010$, Mature vs. Geriatric group: $p < 0.001$; Temporal GL: Controls vs. Mature Group: $p = 0.069^{\#}$, Controls vs. Senior group: $p = 0.002$, Controls vs. Geriatric group: $p < 0.001$, Mature vs. Senior group: $p = 0.043$, Mature vs. Geriatric group: $p = 0.002$; Hippocampal GM: Controls vs. Mature Group: $p = 0.044$, Controls vs. Senior group: $p = 0.008$, Controls vs. Geriatric group: $p < 0.001$, Mature vs. Geriatric group: $p = 0.004$; Hippocampal WM: Controls vs. Mature Group: $p = 0.021$, Controls vs. Senior group: $p = 0.005$, Controls vs. Geriatric group: $p < 0.001$, Mature vs. Geriatric group: $p = 0.006$; Hippocampal GL: Controls vs. Mature Group: $p = 0.066^{\#}$, Controls vs. Senior group: $p = 0.002$, Controls vs. Geriatric group: $p < 0.001$, Mature vs. Senior group: $p = 0.036$, Mature vs. Geriatric group: $p = 0.002$; Frontal GM: Controls vs. Mature Group: $p = 0.078^{\#}$, Controls vs. Senior group: $p = 0.003$, Controls vs. Geriatric group: $p < 0.001$, Mature vs. Senior group: $p = 0.054^{\#}$, Mature vs. Geriatric group: $p = 0.001$; Frontal WM: Controls vs. Mature Group: $p = 0.032$, Controls vs. Senior group: $p = 0.006$, Controls vs. Geriatric group: $p < 0.001$, Mature vs. Geriatric group: $p = 0.007$; Frontal GL: Controls vs. Mature Group: $p = 0.032$, Controls vs. Senior group: $p = 0.015$, Controls vs. Geriatric group: $p < 0.001$, Mature vs. Geriatric group: $p = 0.005$, Senior vs. Geriatric group: $p = 0.056^{\#}$; Cerebellar GM: Controls vs. Mature Group: $p = 0.051^{\#}$, Controls vs. Senior group, $p = 0.005$; Controls vs. Geriatric group: $p < 0.001$, Mature vs. Geriatric group: $p = 0.002$; Cerebellar WM: Controls vs. Mature Group: $p = 0.031$, Controls vs. Senior group: $p = 0.012$, Controls vs. Geriatric group: $p < 0.001$, Mature vs. Geriatric group: $p < 0.001$, Senior vs. Geriatric group: $p = 0.017$; Cerebellar GL: Controls vs. Mature Group: $p = 0.093^{\#}$, Controls vs. Senior group: $p = 0.002$, Controls vs. Geriatric group: $p < 0.001$, Mature vs. Senior group: $p = 0.035$, Mature vs. Geriatric group: $p < 0.001$.

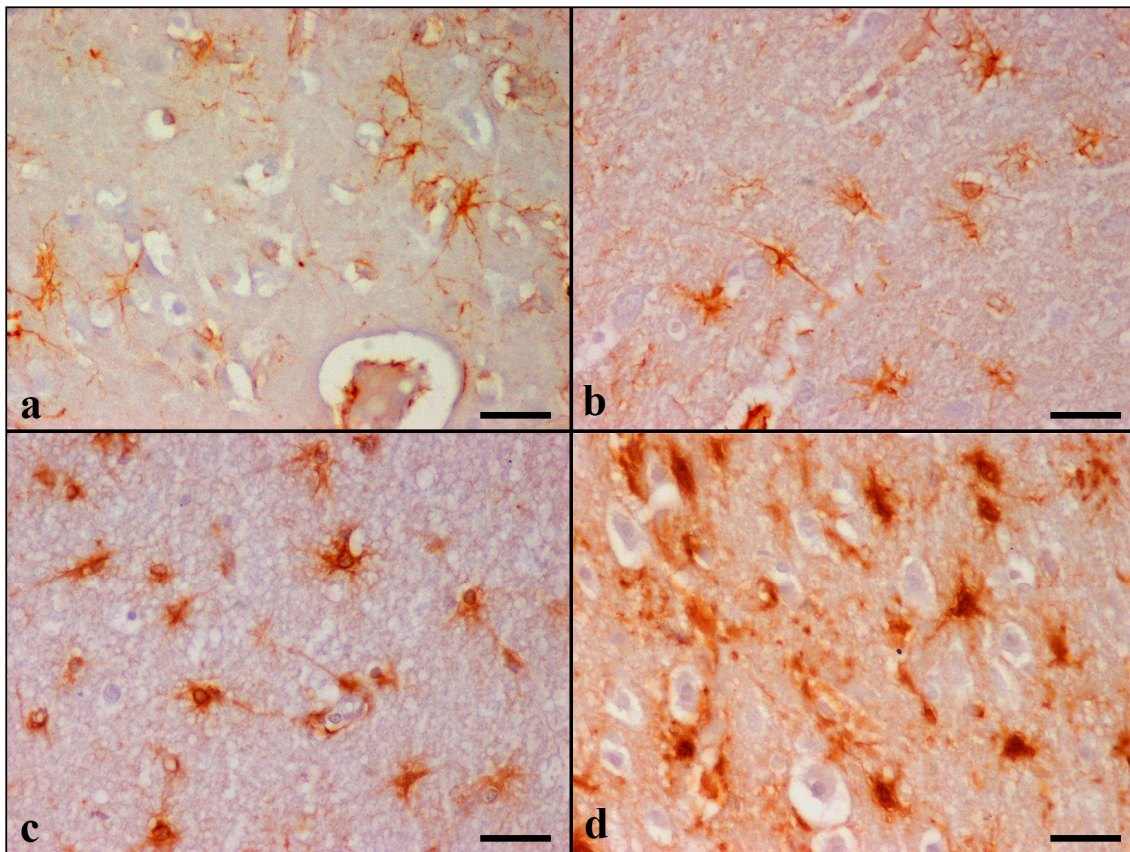


Figure 3. Tissue sections from temporal lobes of cats positively stained for GFAP. (a) Case No 2 aged 2 years old: grade 0 in temporal GM, (b) Case No 13 aged 9 years old: grade 1 in temporal WM, (c) Case No 19 aged 11 years old: grade 2 in temporal WM, (d) Case No 27 aged 17 years old: grade 3 in temporal GM. IHC, DAB chromogen, hematoxylin counterstain. (a–d) Bar = 25 μ m.

GFAP-immunopositive astrocytes were observed in layers I–VI in 22 cases, in layers I–II in 3 cases (case Nos 9, 13, and 14), and throughout layers I–IV in 2 cases (case Nos 7 and 10) in the cerebral cortices. Increased GFAP immunoreactivity was primarily noticed in the hilar astrocytes of the dentate gyrus of the hippocampus and in all cerebellar cortical layers and white matter. Control cats had grade 0, and all 27 aged cats presented all three grades on combined evaluation. Both the morphological alterations and the cell density were more severe in the Geriatric group (most of the animals were evaluated as grade 3 for the majority of the variables).

A β deposition scoring in the examined regions of all aged animals is illustrated in Tables 8 and S5. Domestic cats at an age above 7 years old showed A β pathology. None of the cat brains included in the Controls was positively stained for A β . Immunostaining for A β peptide revealed extracellular deposits forming two types of senile plaques (SPs) in the extracellular space: diffuse granular, which was the most common type observed, and stellate, which was rarely detected. The diffuse type was further divided into two subtypes: condensed and “cloud-like” (Figure 4).

The condensed subtype was characterized by well-circumscribed dense spherical accumulation of A β -positive antigenic material. Morphologically, they had an immunoreactive core and a less well-outlined crown. Degenerating and/or necrotic neurons, glial cells, and blood vessels were occasionally observed in the center of condensed plaques.

On the contrary, “cloud-like” plaques had sparse homogeneous distribution, an irregular to round shape, and granular texture. They were ill defined and variably sized: from small to extremely large deposits.

Table 8. Scoring of A β immunolabeling in the brain of cats of different ages.

Investigated Parameter	Grading Score	Groups				Significance (Chi Square)
		Controls	Mature	Senior	Geriatric	
Temporal leptomeningeal CAA	0	100% (3)	0%	0%	0%	$p < 0.001$
	1	0%	50% (6)	14.3% (1)	62.5% (5)	
	2	0%	41.7% (5)	71.4%	25% (2)	
	3	0%	8.3% (1)	14.3% (1)	12.5% (1)	
	Total	100% (3)	100% (12)	100% (7)	100% (8)	
Temporal GM and WM CAA	0	100% (3)	0%	0%	0%	$p < 0.001$
	1	0%	41.7% (5)	71.4%	87.5% (7)	
	2	0%	25% (3)	14.3% (1)	0%	
	3	0%	33.3% (4)	14.3% (1)	12.5% (1)	
	Total	100% (3)	100% (12)	100% (7)	100% (8)	
Temporal GM neurons	0	100% (3)	33.3% (4)	42.9% (3)	75% (6)	$p = 0.095$ #
	1	0%	66.7% (8)	57.1% (4)	25% (2)	
	2	0%	0%	0%	0%	
	3	0%	0%	0%	0%	
	Total	100% (3)	100% (12)	100% (7)	100% (8)	
Temporal GM and WM SPs	0	100% (3)	50% (6)	0%	0%	$p < 0.001$
	1	0%	25% (3)	14.2% (1)	0%	
	2	0%	0%	42.9% (3)	0%	
	3	0%	25% (3)	42.9% (3)	100% (8)	
	Total	100% (3)	100% (12)	100% (7)	100% (8)	
Hippocampal neurons	0	100% (3)	8.3% (1)	14.3% (1)	25% (2)	$p = 0.002$
	1	0%	83.4% (10)	28.6% (2)	25% (2)	
	2	0%	8.3% (1)	57.1% (4)	50% (4)	
	3	0%	0%	0%	0%	
	Total	100% (3)	100% (12)	100% (7)	100% (8)	
Hippocampal SPs	0	100% (3)	83.3% (10)	71.4%	25% (2)	Non-significant
	1	0%	16.7% (2)	28.6% (2)	37.5% (3)	
	2	0%	0%	0%	12.5% (1)	
	3	0%	0%	0%	25% (2)	
	Total	100% (3)	100% (12)	100% (7)	100% (8)	
Thalamic neurons	0	100% (3)	16.7% (2)	14.3% (1)	37.5% (3)	0.029
	1	0%	8.3% (1)	85.7% (6)	62.5% (5)	
	2	0%	0%	0%	0%	
	3	0%	0%	0%	0%	
	Total	100% (3)	100% (12)	100% (7)	100% (8)	
Thalamic SPs	0	100% (3)	100% (12)	71.4% (5)	37.5% (3)	$p = 0.092$ #
	1	0%	0%	0%	12.5% (1)	
	2	0%	0%	0%	25% (2)	
	3	0%	0%	28.6% (2)	25% (2)	
	Total	100% (3)	100% (12)	100% (7)	100% (8)	

Table 8. Cont.

Investigated Parameter	Grading Score	Groups				Significance (Chi Square)
		Controls	Mature	Senior	Geriatric	
Striatal neurons	0	100% (3)	25% (3)	28.6% (2)	37.5% (3)	Non-significant
	1	0%	75% (9)	57.1% (4)	62.5% (5)	
	2	0%	0%	14.3% (1)	0%	
	3	0%	0%	0%	0%	
	Total	100% (3)	100% (12)	100% (7)	100% (8)	
Striatal SPs	0	100% (3)	100% (12)	57.1% (4)	25% (2)	$p = 0.047$
	1	0%	0%	28.6% (2)	37.5% (3)	
	2	0%	0%	0%	25% (2)	
	3	0%	0%	14.3% (1)	12.5% (1)	
	Total	100% (3)	100% (12)	100% (7)	100% (8)	
CPV amyloid deposits	0	100% (3)	0%	0%	0%	$p < 0.001$
	1	0%	50% (6)	14.3% (1)	25% (2)	
	2	0%	33.3% (4)	71.4% (5)	37.5% (3)	
	3	0%	16.7% (2)	14.3% (1)	37.5% (3)	
	Total	100% (3)	100% (12)	100% (7)	100% (8)	
CP epithelial cells	0	100% (3)	0%	0%	0%	$p < 0.001$
	1	0%	33.3% (4)	0%	0%	
	2	0%	41.7% (5)	57.1% (4)	37.5% (3)	
	3	0%	25% (3)	42.9% (3)	62.5% (5)	
	Total	100% (3)	100% (12)	100% (7)	100% (8)	
Frontal leptomenigeal CAA	0	100% (3)	0%	0%	0%	$p < 0.001$
	1	0%	8.3% (1)	0%	0%	
	2	0%	41.7%	28.6% (2)	25% (2)	
	3	0%	50% (6)%	71.4%	75% (6)	
	Total	100% (3)	100% (12)	100% (7)	100% (8)	
Frontal GM and WM CAA	0	100% (3)	8.3% (1)	0%	0%	$p = 0.002$
	1	0%	58.3% (7)	28.6% (2)	25% (2)	
	2	0%	16.7% (2)	42.8% (3)	50% (4)	
	3	0%	16.7% (2)	28.6% (2)	25% (2)	
	Total	100% (3)	100% (12)	100% (7)	100% (8)	
Frontal GM neurons	0	100% (3)	8.3% (1)	0%	25% (2)	$p = 0.021$
	1	0%	75% (9)	85.7% (6)	62.5% (5)	
	2	0%	16.7% (2)	14.3% (1)	12.5% (1)	
	3	0%	0%	0%	0%	
	Total	100% (3)	100% (12)	100% (7)	100% (8)	
Frontal GM and WM SPs	0	100% (3)	58.3% (7)	28.6% (2)	0%	$p < 0.001$
	1	0%	41.7% (5)	28.6% (2)	0%	
	2	0%	0%	14.3% (1)	0%	
	3	0%	0%	28.6% (2)	100% (8)	
	Total	100% (3)	100% (12)	100% (7)	100% (8)	

Table 8. Cont.

Investigated Parameter	Grading Score	Groups				Significance (Chi Square)
		Controls	Mature	Senior	Geriatric	
Cerebellar leptomeningeal CAA	0	100% (3)	8.3% (1)	0%	0%	$p = 0.002$
	1	0%	41.7% (5)	42.8% (3)	12.5% (1)	
	2	0%	16.7% (2)	28.6% (2)	50% (4)	
	3	0%	33.3% (4)	28.6% (2)	37.5% (3)	
	Total	100% (3)	100%	100%	100%	
Cerebellar GM and WM CAA	0	100% (3)	8.3% (1)	0%	0%	$p < 0.001$
	1	0%	50% (6)	28.6% (2)	12.5% (1)	
	2	0%	16.7% (2)	57.1% (4)	62.5% (5)	
	3	0%	25% (3)	14.3% (1)	25% (2)	
	Total	100% (3)	100% (12)	100% (7)	100% (8)	
Cerebellar GM and DN neurons	0	100% (3)	8.3% (1)	0%	0%	$p < 0.001$
	1	0%	91.7% (11)	100% (7)	75% (6)	
	2	0%	0%	0%	25% (2)	
	3	0%	0%	0%	0%	
	Total	100% (3)	100% (12)	100% (7)	100% (8)	

Kruskal–Wallis test. Temporal leptomeningeal CAA: Controls vs. Mature Group: $p = 0.008$, Controls vs. Senior group: $p < 0.001$, Controls vs. Geriatric group: $p = 0.020$; Temporal GM and WM CAA: Controls vs. Mature Group: $p < 0.001$, Controls vs. Senior group: $p = 0.012$, Controls vs. Geriatric group: $p = 0.026$; Temporal GM and WM SPs: Controls vs. Senior group: $p = 0.020$, Controls vs. Geriatric group: $p < 0.001$, Mature vs. Senior group: $p = 0.077^{\#}$, Mature vs. Geriatric group: $p = 0.001$; Hippocampal neurons: Controls vs. Mature Group: $p = 0.045$, Controls vs. Senior group: $p = 0.006$, Controls vs. Geriatric group: $p = 0.014$, Hippocampal SPs: Controls vs. Geriatric group: $p = 0.015$, Mature vs. Geriatric group: $p = 0.004$, Senior vs. Geriatric group: $p = 0.032$; Thalamic neurons: Controls vs. Mature Group: $p = 0.006$, Controls vs. Senior group: $p = 0.008$, Controls vs. Geriatric group: $p = 0.048$; Thalamic SPs: Controls vs. Geriatric group: $p = 0.041$, Mature vs. Geriatric group: $p = 0.002$; Striatal SPs: Controls vs. Geriatric group: $p = 0.019$, Mature vs. Senior group: $p = 0.060^{\#}$, Mature vs. Geriatric group: $p < 0.001$; CPV amyloid deposits: Controls vs. Mature Group: $p = 0.018$, Controls vs. Senior group: $p = 0.005$, Controls vs. Geriatric group: $p = 0.002$; CP epithelial cells: Controls vs. Mature Group: $p = 0.028$, Controls vs. Senior group: $p = 0.004$, Controls vs. Geriatric group: $p < 0.001$, Mature vs. Geriatric group: $p = 0.065^{\#}$; Frontal leptomeningeal CAA: Controls vs. Mature Group: $p = 0.010$, Controls vs. Senior group: $p = 0.003$, Controls vs. Geriatric group: $p = 0.002$; Frontal GM and WM CAA: Controls vs. Mature Group: $p = 0.035$, Controls vs. Senior group: $p = 0.004$, Controls vs. Geriatric group: $p = 0.003$; Frontal GM neurons: Controls vs. Mature Group: $p = 0.003$, Controls vs. Senior group: $p = 0.004$, Controls vs. Geriatric group: $p = 0.023$; Frontal GM and WM SPs: Controls vs. Mature Group: $p = 0.046$, Controls vs. Senior group: $p = 0.078^{\#}$, Controls vs. Geriatric group: $p < 0.001$, Mature vs. Geriatric group: $p < 0.001$, Senior vs. Geriatric group: $p = 0.037$; Cerebellar leptomeningeal CAA: Controls vs. Mature Group: $p = 0.017$, Controls vs. Senior group: $p = 0.018$, Controls vs. Geriatric group: $p = 0.003$; Cerebellar GM and WM CAA: Controls vs. Mature Group: $p = 0.024$, Controls vs. Senior group: $p = 0.011$, Controls vs. Geriatric group: $p = 0.002$; Cerebellar GM and DN neurons: Controls vs. Mature Group: $p = 0.001$, Controls vs. Senior group: $p < 0.001$, Controls vs. Geriatric group: $p < 0.001$.

Finally, stellate plaques were characterized by a dense center from which fibrils of A β 42 were radiating to the periphery. Radiating fibrils had lengths and thicknesses of varying sizes, giving a star-like appearance.

SPs were found in 21/27 aged cats over 7 years old in gray matter, and in 12 of them, there were also deposits in white matter. They were distributed within layers III to VI of the cerebral cortex. Plaque formation was also observed in 10 cats over 9 years old in the hippocampus, in 7 cases over 12 years old in the thalamus, and in 9 cats over 12 years old in the striatum. No plaque formation was detected in the sections of cerebellum.

Diffuse plaques of both subtypes were observed in all 21 aged cats, which revealed plaque formation, except in case No 15, where there was only one condensed plaque located in the VI cortical layer of the temporal lobe. Stellate plaques were found in eight cats over 14 years old (case Nos 21, 23–25, and 27–30). In particular, cats of the Geriatric group (15 to 20 years old) had higher scores regarding extracellular deposits. The severity of pathology

and the number of cats with SPs increased with age (frontal and temporal GM and WM SPs: $p < 0.001$; thalamic SPs: $p = 0.092$ #; and striatal SPs: $p = 0.047$).

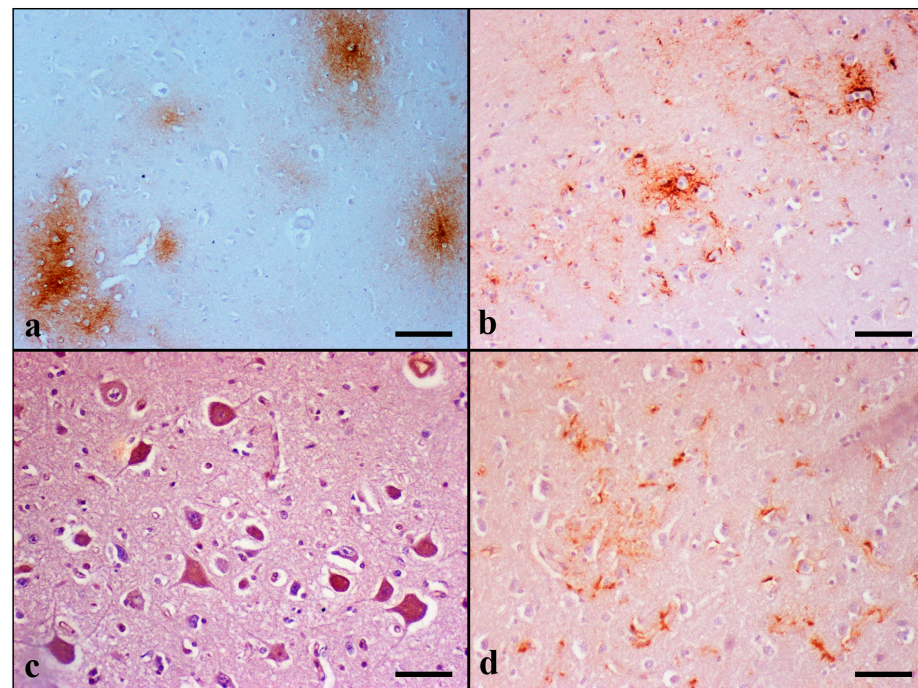


Figure 4. A β 42 immunolabeling in the brain of aged cats. (a) Condensed and cloud-like amyloid plaques within the neuropil of the temporal cortex. Within condensed plaques can be observed intact non-stained neurons (case No 6). (b) Two A β 42-positive stellate plaques can be observed in the neuropil of the temporal cortex. Glial cells with long and thin or short and thick cytoplasmic processes, probably reactive astrocytes, are also positively stained (case No 29). (c) Intense cytoplasmic A β 42 immunostaining in Betz neurons (layer V) of the frontal cortex (case No 4). (d) A β 42 is occasionally present in the cytoplasm and cytoplasmic processes of astrocytes within the frontal cortex. A cloud-like plaque surrounded by positively stained astrocytes is obvious (case No 24). IHC, DAB chromogen, hematoxylin counterstain. (a) Bar = 100 μ m, (b–d) Bar = 50 μ m.

In addition to plaques, A β -positive staining forming band-like deposition was also found in cats over 12 years old. They were distributed within the hippocampal dentate molecular layer and stratum lacunosum-moleculare (case Nos 27, 29, and 30); hippocampal alveus, fimbria, and stratum oriens (case No 28); temporal cortical layer V to VI (case Nos 18, 19, 26, 29, and 30); and both in the frontal and temporal cortex in layers V–VI (case Nos 20, 21, 23–25, 27, and 28).

A β immunoreactivity was also detected in the wall of the LV, CPV, cerebral and cerebellar vessels, and around the wall of cerebral capillaries. Intracytoplasmic accumulation of A β was detected in the neurons of the cerebral cortex, hippocampus, thalamus, striatum, and cerebellum. Increased A β 42 immunostaining was noticed within layers III to VI of the cerebral cortex, in the pyramidal layer of the CA, and Purkinje and Golgi type II cells of the cerebellar cortex. Additionally, CP epithelial cells in all elderly cats showed A β 42 immunoreactivity.

Besides neuronal accumulation, astrocytes also showed intracytoplasmic immunolabeling of A β . This was observed in the frontal and temporal lobes and the cerebellum in six aged cats (case Nos 5, 12, 21, 24, 26, and 28).

3.4. ICP-MS Metal Analysis

The levels of iron and zinc in the analyzed brain tissues are reported in Table 9. The highest iron and zinc levels were detected in case Nos 21 and 26, while the lowest was detected in case No 1. For both metals, no statistical significance was noticed among the

age groups ($p > 0.1$). However, increasing age was associated with a mild increase in iron levels in the brain, as illustrated in Figure 5. Regarding zinc, a mild numerical increase in the Mature and Senior groups was displayed compared to the Controls (Figure 5). The Geriatric group concentration of zinc was similar to the Controls.

Table 9. Iron and zinc concentrations in brain tissues of all cats.

Groups	Case No	Fe ($\mu\text{g/g}$)	Zn ($\mu\text{g/g}$)
Controls	1	175.2	29.9
	2	225.3	18.5
	3	310.8	16.1
Mature	4	264.6	36.7
	5	252.6	17.9
	6	270.4	26.8
	7	269.6	28.8
	8	264.6	17.8
	9	313	18.7
	10	267	22.5
	11	333.8	35.8
	12	488.8	45.9
	13	248.3	19.4
	14	276.4	24.8
	15	243	31.59
Senior	16	227.8	32.38
	17	208.2	18.2
	18	268.7	24.8
	19	238.7	29.4
	20	318	22.2
	21	934.6	1202
	22	326	25.8
Geriatric	23	301.7	19.9
	24	260.7	18.4
	25	253.6	17
	26	1374.3	2057.9
	27	395.3	31.4
	28	226	18.9
	29	341.8	24.3
	30	329.3	26.7

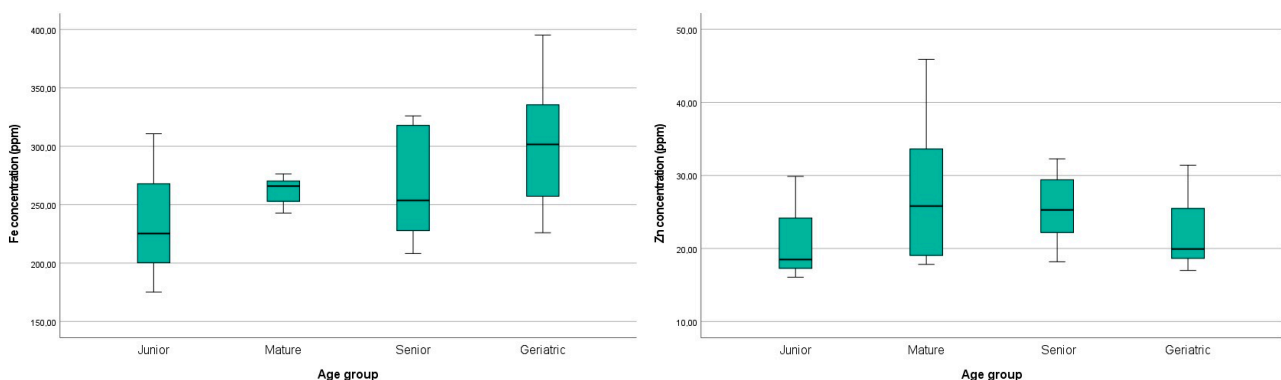


Figure 5. The results were not statistically significant ($p > 0.1$) for both iron and zinc. A mild age-dependent numerical increase in iron and mildly elevated zinc concentration in the Mature and Senior groups were noticed.

4. Discussion

An aging brain is strongly associated with several functional and morphological alterations. Brain biometal dyshomeostasis, such as iron and zinc, contributes to increased

oxidative stress, which is related to severe neuronal damage in normal aging and neurodegenerative diseases in both humans and animals [26,37]. In the present study, we investigated the association of age-related histopathology, including A β deposition, with brain MT-I/II and metal ion accumulation.

Most of the histopathological alterations demonstrated using H-E appeared to increase with age ($p < 0.1$), as has been described in previous reports on aged cats [4,6,7,27]. Neuronophagia, satellitosis, and chromatolysis were more severe in animals over 17 years old. Neuronal necrosis and loss observed in the cerebellum mostly affected Purkinje neurons and then Golgi type II cells, dentate nucleus, and granule cells. Interestingly, regional complete Purkinje cell loss was observed and sometimes alongside reduced granule cell density (case Nos 20, 23, 24, 27, and 29). This finding is in agreement with Brellou (2006) who further noticed reduced Golgi type II cells [6]. Furthermore, Zhang et al. (2006) observed a severe loss of neurons in the cerebellar molecular layer of aged cats [27]. In addition, axons exhibited degenerative changes characterized by myelin sheath rupture and segmental loss and the presence of vesicular formations. The latter observation was more prominent in the Geriatric group. Another observation worth mentioning, which has also been mentioned by Brellou (2006), is that while the number of Lafora-like bodies was greatly increased in aged cats over 11 years old, they showed decrement in size with age [6].

In addition to the age-related changes detected by several authors, Brellou (2006) also observed spherical-to-ovoid structures stained exclusively with H-E staining in cerebral cortical gray and white matter and in the cerebellar molecular layer and dentate nuclei of aged cats [6]. Interestingly, we detected similar H-E-positive bodies in the cerebral GM and WM matter, the cerebellar molecular layer, and the dentate nuclei of 14 cats over 8 years old. In both cortices, the H-E-positive bodies were distributed within layers I and II. The above bodies were detected only with H-E staining, and an age-dependent increase was noted ($p = 0.014$). Further investigation could be undertaken to clarify the origin and role of these structures in the aged feline CNS.

Regarding brain iron accumulation, we performed the Perl's/DAB staining method, a modified Perl's staining described by Meguro et al. (2007) [33]. The Meguro modification primarily stains Fe³⁺, but also Fe²⁺, and is widely used in order to achieve higher sensitivity [33]. DAB-enhanced Perl's methods have been applied in the brain of aged dogs [38], in the brain of aged rats [39,40], in human brain tissue with AD pathology [41–43], in the brain of aged wild-type mice [44], and in a mouse model (APP/PS1) of AD [45].

Previously, researchers have observed the extracellular deposition of iron and, particularly, the formation of plaques stained with Perl's/DAB in the cortex, hippocampus, cerebellum, caudoputamen, and thalamic nuclei of mice and in the frontal cortex of AD patients [41,43,45]. Moreover, Kim E. et al. (2021) noticed the presence of iron-containing A β plaques throughout the cerebral cortex, hippocampus, and thalamus of rodents [46]. According to Sands et al. (2016), the IPS demonstrated either dense core staining or sometimes diffuse. This is in line with our observations in cats regarding both condensed and diffuse IPs in the same regions [45].

Along with plaques, prior research has indicated iron-myelin-associated staining in the cerebellar white matter of rats; in the globus pallidus, ventral pallidum, basal ganglia, and substantia nigra of mice; in the globus pallidus of aged dogs; and in the frontal white matter and myelin-rich cortical layers IV and V of human AD patients [38,40,41,43,45,47]. Similarly, in our study, iron-myelin-associated staining was also observed for the first time in the aging feline brain located in the frontal, temporal, and cerebellar white matter; thalamus; and hippocampal fimbria.

Sands et al. (2016) also noticed punctate staining in neurons located in the cortex, CA hippocampal layer, and dentate gyrus [45]. Neurons occasionally revealed nuclear, nucleolar, and/or cytoplasmic staining, without describing, in detail, the exact cellular distribution. Meguro et al. (2008) also demonstrated cytoplasmic and nuclear neuronal staining in the cerebellar nuclei and cortex, globus pallidus, and in many brain stem structures in a rat brain [40]. Similarly, our results showed nucleolar, nuclear, and/or

cytoplasmic staining within neurons delocated in the cerebral cortices, the hippocampal stratum pyramidale layer, the dentate gyrus, the thalamus, and the cerebellum. However, in our study, we demonstrated that the nucleolus was the primary iron-labeled site in the aged feline brain. Previous studies have also demonstrated that the neuronal nucleolus is a “hot spot” for iron, showing a higher concentration than the nucleus and the perikaryon in rat brains [48,49].

It has been suggested that aging might result in an increased concentration of total iron and lead to the accumulation of iron in neurons and glial cells in humans [14]. Particularly, glial cells also exhibit Perl's/DAB staining. Earlier studies have shown iron-positive oligodendrocytes, astroglia, and microglia in aged rats, mice, dogs, and humans [38,40–43,45]. In our study, no double staining was performed to demonstrate simultaneous glial cell type and iron accumulation. However, based on cell morphology, including the detection of long cytoplasmic processes, these cells were identified either as astrocytes or as activated microglia.

It has been widely acknowledged that essential metal dyshomeostasis is strongly correlated with aging [11,13,14,16,17,26]. Increased iron concentrations have been frequently associated with age in the brain of humans, rats, mice, *O. degus*, and dogs [11,14,38–40,50,51]. In the present study, a statistically significant age-dependent increment in iron accumulation was demonstrated using Perl's/DAB staining, exclusively regarding plaque load in the frontal grey and white matter ($p = 0.088$ #) and the thalamus ($p = 0.025$), as well as myelin-associated iron in the cerebellum ($p = 0.002$). However, our findings using ICP-MS did not show statistically significant differences regarding iron levels among the age groups ($p > 0.1$), and iron concentrations showed a minor age-related increase, as shown in Figure 5.

Concerning zinc levels, there is scientific controversy for the age-dependent increment in zinc concentration in the brain using ICP-MS analysis. While Takahashi et al. (2001) showed that zinc levels did not vary with age in rodents, Zatta et al. (2008) detected an age-related significant increase in zinc in the cerebellum and thalamus in cattle [26,52]. Previous reports have demonstrated a significant increment in zinc concentrations in the cortex and hippocampus of *O. degus* and in the globus pallidus of mice. On the contrary, zinc levels were not significantly increased with age in the hippocampus of mice [11,50]. Our ICP-MS results did not show statistically significant differences regarding zinc levels among the age groups ($p > 0.1$). However, higher levels of zinc were observed in the cats of the Mature and Senior group aged from 7 to 14 years old compared to those of the Controls and Geriatric groups.

Metal concentration analysis with ICP-MS was not determined regionally but in a total of five regions. As a result, it was not feasible to examine the precise distribution and calculate the concentration of these essential metals in each specific region separately in the feline brain. But, as regards iron deposits in situ in several areas of the feline brain, the detailed distribution, morphology (types), and localization was achieved with Perl's/DAB staining. The latter was proven to be a precious method, as for many other authors who studied human AD, mice, and canine brains [38,41,43–45].

Another constant finding in the present study worth mentioning was the intense expression of MT-I/II in astroglia, a metalloprotein involved in metal binding and protection against reactive oxygen species [20,22]. Although MT-I/II is primarily produced by astrocytes [53], other cell types also show MT-I/II expression [21,54]. Similarly, our immunohistochemical results showed predominantly MT-I/II immunoreactive astrocytes in addition to neurons, LCs, CP cells, and ependymal cells, as well as endothelial cells. Furthermore, MT-I/II expression was also demonstrated in vascular tunica media.

Earlier studies have also noticed MT-I/II immunolabeling in domestic animals. Shimada et al. (1998) demonstrated increased MT-I/II astrocytic immunostaining with age in the intact brain areas of 13 dogs with neurological signs [23]. Zatta et al. (2008) found MT-I/II immunoreactive astrocytes in the cerebellum, frontal and parietal cortex, and ependymal cells in the brain of both young and aged cattle. However, they did not note any significant difference in the distribution of MT in association with age [26]. Our findings are

almost in accordance with those of Kojima et al. (1999), who found MT-I/II immunopositive astrocytes, both in the cytoplasm and nucleus, ependymal cells, and CP epithelial cells in the brain of aged dogs [24], a finding also observed in monkeys [55], rats [56,57], and mice [56,58]. Positive astrocytes were distributed in the cerebral cortical layers from III to V, white matter, hippocampus, thalamus, periventricular area, and around the blood vessels of each region [24]. Morita et al. (2005) also demonstrated the expression of MT-I/II, mainly in astrocytes around the blood vessels of aged dogs [38]. The latter observation regarding the perivascular presence of astrocytes combined with the fact that astrocytes are an essential part of the blood–brain barrier and that they ensheath blood vessels indicates that MT-I/II plays a pivotal role, acting as a barrier for dysregulated metal uptake.

We further observed MT-I/II immunoreactivity in neurons of all regions examined. Specifically, neuronal MT-I/II expression has scarcely been demonstrated in reports on humans, mice, rats, and sheep [20,21]. In our study, MT-I/II-positive staining was demonstrated in a noticeable number of cats (14 cases). This finding in the feline brain might be attributed to cytoplasmic MT-I/II extracellular release and then its internalization by neurons, eventually promoting neurite outgrowth and neuronal survival (as reviewed in [21]).

In conclusion, statistical analysis revealed a significant increment in MT-I/II expression. All the variables examined, except MT-I/II immunoreactivity in the temporal and frontal leptomeningeal and GM and WM blood vessels, were statistically significant ($p < 0.1$). Taking into consideration the fact that we compared different age groups, it might be concluded that MT-I/II expression is positively correlated with age in the feline brain. Our results agree with Mocchegiani et al. (2001), who also observed increased MT-I/II immunoreactivity in the brain of old rats and proposed MT-I/II as a potential marker of aging [25].

In the feline brain, a correlation between amyloid beta deposition and increasing age has been widely documented [59]. In the current study, both intracellular and extracellular A β deposits were observed. The latter were detected from the age of 7 years old. Previous studies of feline A β pathology have reported deposits in cats over 7.5 years old [6,60–62], but in a recent study, the youngest cat was 4 years old [8]. However, additional data regarding the animal's detailed history were not mentioned.

Interestingly, among the brain regions we examined, the cerebellum showed the lowest load of A β , and extracellular deposits were absent. Cerebellar A β deposits have been reported in aged cats [6,8]. According to Thal et al. (2002), the cerebellum is involved in end-stage AD [63]. In the present study, it is likely that our cases might have developed cerebellum deposition if they had lived longer [8].

Although neurons were assumed for a long time as the exclusive cell type capable of producing A β , additional studies have indicated that astrocytes also generate beta amyloid [64–69]. Both cell types express BACE1 (β -site APP cleaving enzyme 1), which is indispensable for A β production, and its expression can be increased due to cellular stress [30,68]. Age-dependent astrogliosis has been reported in animals including dogs [23,70], cattle [71], horses [72], and cats [6,28]. Accordingly, in the present study, the identification of GFAP-positive astrocytes and further classification into four separate grades were performed based on Boos et al. (2021), and a statistically significant age-related increase in size and number of positive astrocytes was observed [35]. Given that astrocytes outnumber neurons in the brain and reactive astrogliosis is associated with aging, these could lead to astrocyte contribution in A β production in aged humans and/or animals [30,68]. In our study, we documented, for the first time, the intracytoplasmic immunohistochemical detection of A β in astrocytes in the aged feline brain.

A β extracellular deposits have also been related to high levels of iron and zinc ions in AD [14,15,29,43,46]. Previous research has demonstrated a positive correlation between iron accumulation and A β plaques in the frontal cortex of humans with AD and throughout the brain of rodents [43,46]. Increased total brain iron has been associated with early A β plaque formation in a mouse model of AD [73]. Furthermore, studies have shown that

MT-I/II is expressed in high levels in AD and is also associated with A β plaques in the hippocampus of AD animal models [21]. In the current study, two cases (case Nos 21 and 26; 14 and 17 years old, respectively) showed the highest brain concentration of both iron and zinc among the animals when analyzed with ICPMS. Interestingly, those cats also had a very high A β plaque load in the temporal and frontal lobes. Particularly, case No 21 had 125 plaques in the frontal lobe and 112 SPs in the temporal lobe, while in case No 26, 62 and 99 SPs were found in the same regions, respectively. The same cats also displayed histochemically high iron plaque burden and high expression of MT-I/II. These data suggest that there might be a positive correlation between iron and zinc levels, as well as MT-I/II expression, with A β extracellular deposition in the brain of aged cats.

To the authors' knowledge, this is the first study to investigate the feline brain for MT-I/II expression, iron and zinc ion concentrations and iron ion distribution as well. Also, an attempt was made to further compare these findings with age-related histopathology including A β deposits. In light of the evidence raised, we strongly suggest that cats merit further investigation as a natural animal model of brain aging and neurodegenerative diseases.

Supplementary Materials: The following supporting information can be downloaded at <https://www.mdpi.com/article/10.3390/brainsci13071115/s1>. Table S1: Histopathological scoring of age-related brain lesions in mature, senior, and geriatric cats; Table S2: Iron deposition scoring in the brains of aged cats; Table S3: Scoring of MT-I/II immunolabeling in cats of different ages; Table S4: Grading of GFAP immunolabeling; Table S5: Scoring of A β immunolabeling in the brain of cats of different ages; Figure S1: Condensed plaques characterized by spherical accumulation of iron with dense core and diffuse, poorly delimited IPs. Neurons and glial cells are also stained. Perl's/DAB. Bar = 50 μ m.

Author Contributions: Conceptualization, E.P.A. and G.D.B.; methodology, G.D.B., I.V., N.R. and E.P.A.; formal analysis, G.D.B., E.P.A., I.V. and N.R.; investigation, E.P.A., G.D.B., N.R., I.V. and E.M.; writing—original draft preparation, E.P.A.; writing—review and editing, G.D.B., I.V., N.R. and E.M.; supervision, G.D.B. All authors have read and agreed to the published version of the manuscript.

Funding: This study is part of a PhD thesis. The implementation of the doctoral thesis was co-financed by Greece and the European Union (European Social Fund—ESF) through the Operational Programme Human Resources Development, Education, and Lifelong Learning in the context of the Act: Enhancing Human Resources Research Potential by undertaking Doctoral Research, Sub-action 2: IKY Scholarship Programme for PhD candidates in the Greek Universities, granted to E.P.A. (funding number: 2022-050-0502-52525).

Institutional Review Board Statement: Not applicable.

Informed Consent Statement: Informed consent was obtained from all cat owners involved in this study.

Data Availability Statement: Additional data are available from the corresponding author upon request.

Acknowledgments: We would like to thank Simeon Karolidis, Dimitrios Katsiaflakas, and George Georgakis for their contribution to the ICP-MS analysis at the Chemical Department, 3rd Army Veterinary Hospital. We are grateful to Ilias Giannenas of the Laboratory of Nutrition for providing technical equipment and to the PhD student Tilemachos Mantzios for his valuable assistance in the statistical analysis.

Conflicts of Interest: The authors declare no conflict of interest.

References

1. O'Neill, D.G.; Church, D.B.; McGreevy, P.D.; Thomson, P.C.; Brodbelt, D.C. Longevity and mortality of cats attending primary care veterinary practices in England. *J. Feline Med. Surg.* **2015**, *17*, 125–133. [[CrossRef](#)] [[PubMed](#)]
2. Emamzadeh, F.N.; Surguchov, A. Parkinson's Disease: Biomarkers, Treatment, and Risk Factors. *Front. Neurosci.* **2018**, *12*, 612. [[CrossRef](#)]
3. Dror, Y.; Stern, F.; Gomori, M.J. Vitamins in the prevention or delay of cognitive disability of aging. *Curr. Aging Sci.* **2014**, *7*, 187–213. [[CrossRef](#)]

4. Youssef, S.A.; Capucchio, M.T.; Rofina, J.E.; Chambers, J.K.; Uchida, K.; Nakayama, H.; Head, E. Pathology of the aging brain in domestic and laboratory animals; and animal models of human neurodegenerative diseases. *Vet. Pathol.* **2016**, *53*, 327–348. [[CrossRef](#)]
5. Summers, B.A.; Cummings, J.F.; de Lahunta, A. *Veterinary Neuropathology*, 1st ed.; Mosby: St. Louis, MO, USA, 1995.
6. Brellou, D.G. Studies on the Histopathological Changes and Presence of Amyloid β Protein ($A\beta$) Deposits in the Aged Feline Brain. Ph.D. Thesis, Aristotle University of Thessaloniki, Thessaloniki, Greece, 2006. [[CrossRef](#)]
7. Vite, C.H.; Head, E. Aging in the canine and feline brain. *Vet. Clin. N. Am. Small Anim. Pract.* **2014**, *44*, 1113–1129. [[CrossRef](#)] [[PubMed](#)]
8. Sordo, L.; Martini, A.C.; Houston, E.F.; Head, E.; Gunn-Moore, D. Neuropathology of Aging in Cats and its Similarities to Human Alzheimer's Disease. *Front. Aging* **2021**, *2*, 684607. [[CrossRef](#)]
9. Farrall, A.J.; Wardlaw, J.M. Blood-brain barrier, ageing and microvascular disease—Systematic review and meta-analysis. *Neurobiol. Aging* **2009**, *30*, 337–352. [[CrossRef](#)]
10. Montagne, A.; Barnes, S.R.; Sweeney, M.D.; Halliday, M.R.; Sagare, A.P.; Zhao, Z.; Toga, A.W.; Jacobs, R.E.; Liu, C.Y.; Amezcua, L.; et al. Blood-brain barrier breakdown in the aging human hippocampus. *Neuron* **2015**, *85*, 296–302. [[CrossRef](#)]
11. Ashraf, A.; Michaelides, C.; Walker, T.A.; Ekonomou, A.; Suessmilch, M.; Sriskanthanathan, A.; Abraha, S.; Parkes, A.; Parkes, H.G.; Geraki, K.; et al. Regional Distributions of Iron, Copper and Zinc and Their Relationships with Glia in a Normal Aging Mouse Model. *Front. Aging Neurosci.* **2019**, *11*, 351. [[CrossRef](#)]
12. Verkhatsky, A.; Zorec, R.; Rodriguez-Arellano, J.J.; Parpura, V. Neuroglia in Ageing. *Adv. Exp. Med. Biol.* **2019**, *1175*, 181–197. [[CrossRef](#)] [[PubMed](#)]
13. Ijomone, O.K.; Aschner, M. The aging brain, impact of heavy metal neurotoxicity. *Crit. Rev. Toxicol.* **2020**, *50*, 801–814. [[CrossRef](#)] [[PubMed](#)]
14. Ward, R.J.; Zucca, F.A.; Duyn, J.H.; Crichton, R.R.; Zecca, L. The role of iron in brain ageing and neurodegenerative disorders. *Lancet Neurol.* **2014**, *13*, 1045–1060. [[CrossRef](#)] [[PubMed](#)]
15. McCord, M.C.; Aizenman, E. The role of intracellular zinc release in aging, oxidative stress; and Alzheimer's disease. *Front. Aging Neurosci.* **2014**, *6*, 77. [[CrossRef](#)]
16. Walker, T.; Michaelides, C.; Ekonomou, A.; Geraki, K.; Parkes, H.G.; Suessmilch, M.; Herlihy, A.H.; Crum, W.R.; So, P.W. Dissociation between iron accumulation and ferritin upregulation in the aged substantia nigra, attenuation by dietary restriction. *Aging* **2016**, *8*, 2488–2508. [[CrossRef](#)]
17. Frazzini, V.; Rockabrand, E.; Mocchegiani, E.; Sensi, S.L. Oxidative stress and brain aging, is zinc the link? *Biogerontology* **2006**, *7*, 307–314. [[CrossRef](#)] [[PubMed](#)]
18. Kruszewski, M. Labile iron pool, the main determinant of cellular response to oxidative stress. *Mutat. Res.* **2003**, *531*, 81–92. [[CrossRef](#)]
19. Choi, S.; Hong, D.K.; Choi, B.Y.; Suh, S.W. Zinc in the Brain, Friend or Foe? *Int. J. Mol. Sci.* **2020**, *21*, 8941. [[CrossRef](#)]
20. Hidalgo, J.; Aschner, M.; Zatta, P.; Vasák, M. Roles of the metallothionein family of proteins in the central nervous system. *Brain Res. Bull.* **2001**, *55*, 133–145. [[CrossRef](#)]
21. Waller, R.; Murphy, M.; Garwood, C.J.; Jennings, L.; Heath, P.R.; Chambers, A.; Matthews, F.E.; Brayne, C.; Ince, P.G.; Wharton, S.B.; et al. Metallothionein-I/II expression associates with the astrocyte DNA damage response and not Alzheimer-type pathology in the aging brain. *Glia* **2018**, *66*, 2316–2323. [[CrossRef](#)]
22. Vasak, M.; Meloni, G. Chemistry and biology of mammalian metallothioneins. *J. Biol. Inorg. Chem.* **2011**, *16*, 1067–1078. [[CrossRef](#)]
23. Shimada, A.; Yamamura, Y.; Kojima, S.; Morita, T.; Umemura, T. Localization of metallothionein-I and II in hypertrophic astrocytes in brain lesions of dogs. *J. Vet. Med. Sci.* **1998**, *60*, 351–358. [[CrossRef](#)]
24. Kojima, S.; Shimada, A.; Morita, T.; Yamano, Y.; Umemura, T. Localization of Metallothioneins-I&-II and III in the brain of aged dog. *J. Vet. Med. Sci.* **1999**, *61*, 343–349. [[PubMed](#)]
25. Mocchegiani, E.; Giacconi, R.; Cipriano, C.; Muzzioli, M.; Fattoretti, P.; Bertoni-Freddari, C.; Isani, G.; Zambenedetti, P.; Zatta, P. Zinc-bound metallothioneins as potential biological markers of ageing. *Brain Res. Bull.* **2001**, *55*, 147–153. [[CrossRef](#)] [[PubMed](#)]
26. Zatta, P.; Drago, D.; Zambenedetti, P.; Bolognin, S.; Nogara, E.; Peruffo, A.; Cozzi, B. Accumulation of copper and other metal ions; and metallothionein I/II expression in the bovine brain as a function of aging. *J. Chem. Neuroanat.* **2008**, *36*, 1–5. [[CrossRef](#)] [[PubMed](#)]
27. Zhang, C.; Hua, T.; Zhu, Z.; Luo, X. Age-related changes of structures in cerebellar cortex of cat. *J. Biosci.* **2006**, *31*, 55–60. [[CrossRef](#)] [[PubMed](#)]
28. Ozsoy, S.; Hazirolu, R. Age-related changes in cat brains as demonstrated by histological and immunohistochemical techniques. *Revue Med. Vet.* **2010**, *161*, 540–548.
29. Bishop, G.M.; Robinson, S.R.; Liu, Q.; Perry, G.; Atwood, C.S.; Smith, M.A. Iron, a pathological mediator of Alzheimer disease? *Dev. Neurosci.* **2002**, *24*, 184–187. [[CrossRef](#)]
30. Frost, G.R.; Li, Y.M. The role of astrocytes in amyloid production and Alzheimer's disease. *Open Biol.* **2017**, *7*, 170–228. [[CrossRef](#)]
31. Dittmann, J.; Fung, S.J.; Vickers, J.C.; Chuah, M.I.; Chung, R.S.; West, A.K. Metallothionein biology in the ageing and neurodegenerative brain. *Neurotox. Res.* **2005**, *7*, 87–93. [[CrossRef](#)]
32. Vogt, A.H.; Rodan, I.; Brown, M.; Brown, S.; Buffington, C.A.T.; Forman, M.J.L.; Neilson, J.; Sparkes, A. AAFP-AAHA Feline Life Stage Guidelines. *J. Feline Med. Surg.* **2010**, *12*, 43–54. [[CrossRef](#)]

33. Meguro, R.; Asano, Y.; Odagiri, S.; Li, C.; Iwatsuki, H.; Shoumura, K. Nonheme-iron histochemistry for light and electron microscopy, a historical; theoretical and technical review. *Arch. Histol. Cytol.* **2007**, *70*, 1–19. [[CrossRef](#)]
34. Sukhorukova, E.G.; Grigoriev, I.P.; Kirik, O.V.; Alekseeva, O.S.; Korzhevskii, D.E. Intranuclear localization of iron in neurons of mammalian brain. *J. Evol. Biochem. Physiol.* **2013**, *49*, 370–372. [[CrossRef](#)]
35. Boos, G.S.; Failing, K.; Colodel, E.M.; Driemeier, D.; de Castro, M.B.; Bassuino, D.M.; Diomedes Barbosa, J.; Herden, C. Glial Fibrillary Acidic Protein and Ionized Calcium-Binding Adapter Molecule 1 Immunostaining Score for the Central Nervous System of Horses with Non-suppurative Encephalitis and Encephalopathies. *Front. Vet. Sci.* **2021**, *8*, 660022. [[CrossRef](#)]
36. Takahashi, K.; Chambers, J.K.; Takaichi, Y.; Uchida, K. Different A β 43 deposition patterns in the brains of aged dogs, sea lions, and cats. *J. Vet. Med. Sci.* **2022**, *84*, 1563–1573. [[CrossRef](#)]
37. Bolognin, S.; Messori, L.; Zatta, P. Metal ion physiopathology in neurodegenerative disorders. *Neuro. Med.* **2009**, *11*, 223–238. [[CrossRef](#)]
38. Morita, T.; Mizutani, Y.; Sawada, M.; Shimada, A. Immunohistochemical and ultrastructural findings related to the blood–brain barrier in the blood vessels of the cerebral white matter in aged dogs. *J. Comp. Pathol.* **2005**, *133*, 14–22. [[CrossRef](#)] [[PubMed](#)]
39. Kim, J.M.; Ko, S.B.; Kwon, S.J.; Kim, H.J.; Han, M.K.; Kim, D.W.; Cho, S.S.; Jeon, B.S. Ferrous and ferric iron accumulates in the brain of aged Long-Evans Cinnamon rats; an animal model of Wilson’s disease. *Neurosci. Lett.* **2005**, *382*, 143–147. [[CrossRef](#)] [[PubMed](#)]
40. Meguro, R.; Asano, Y.; Odagiri, S.; Li, C.; Shoumura, K. Cellular and subcellular localizations of nonheme ferric and ferrous iron in the rat brain, a light and electron microscopic study by the perfusion-Perls and -Turnbull methods. *Arch. Histol. Cytol.* **2008**, *71*, 205–222. [[CrossRef](#)] [[PubMed](#)]
41. van Duijn, S.; Nabuurs, R.J.; van Duinen, S.G.; Natté, R. Comparison of histological techniques to visualize iron in paraffin-embedded brain tissue of patients with Alzheimer’s disease. *J. Histochem. Cytochem.* **2013**, *61*, 785–792. [[CrossRef](#)]
42. Zeineh, M.M.; Chen, Y.; Kitzler, H.H.; Hammond, R.; Vogel, H.; Rutt, B.K. Activated iron-containing microglia in the human hippocampus identified by magnetic resonance imaging in Alzheimer disease. *Neurobiol. Aging* **2015**, *36*, 2483–2500. [[CrossRef](#)]
43. van Duijn, S.; Bulk, M.; van Duinen, S.G.; Nabuurs, R.J.A.; van Buchem, M.A.; van der Weerd, L.; Natté, R. Cortical Iron Reflects Severity of Alzheimer’s Disease. *J. Alzheimer’s Dis.* **2017**, *60*, 1533–1545. [[CrossRef](#)]
44. Mezzanotte, M.; Ammirata, G.; Boido, M.; Stanga, S.; Roetto, A. Activation of the Hcpidin-Ferroportin1 pathway in the brain and astrocytic-neuronal crosstalk to counteract iron dyshomeostasis during aging. *Sci. Rep.* **2022**, *12*, 11724. [[CrossRef](#)] [[PubMed](#)]
45. Sands, S.A.; Leung-Toung, R.; Wang, Y.; Connelly, J.; LeVine, S.M. Enhanced Histochemical Detection of Iron in Paraffin Sections of Mouse Central Nervous System Tissue, Application in the APP/PS1 Mouse Model of Alzheimer’s Disease. *ASN Neuro* **2016**, *8*, 1759091416670978. [[CrossRef](#)] [[PubMed](#)]
46. Kim, E.; Di Censo, D.; Baraldo, M.; Simmons, C.; Rosa, I.; Randall, K.; Ballard, C.; Dickie, B.R.; Williams, S.C.R.; Killick, R.; et al. In vivo multi-parametric manganese-enhanced MRI for detecting amyloid plaques in rodent models of Alzheimer’s disease. *Sci. Rep.* **2021**, *11*, 12419. [[CrossRef](#)] [[PubMed](#)]
47. Heidari, M.; Gerami, S.H.; Bassett, B.; Graham, R.M.; Chua, A.C.; Aryal, R.; House, M.J.; Collingwood, J.F.; Bettencourt, C.; Houlden, H.; et al. Pathological relationships involving iron and myelin may constitute a shared mechanism linking various rare and common brain diseases. *Rare Dis.* **2016**, *4*, e1198458. [[CrossRef](#)]
48. Fiedler, A.; Reinert, T.; Morawski, M.; Bruckner, G.; Arendt, T.; Butz, T. Intracellular iron concentration of neurons with and without perineuronal nets. *Nucl. Instrum. Methods Phys. Res. B Beam Interact. Mater. At.* **2007**, *260*, 153–158. [[CrossRef](#)]
49. Reinert, A.; Morawski, M.; Seeger, J.; Arendt, T.; Reinert, T. Iron concentrations in neurons and glial cells with estimates on ferritin concentrations. *BMC Neurosci.* **2019**, *20*, 25. [[CrossRef](#)]
50. Braidy, N.; Poljak, A.; Marjo, C.; Rutledge, H.; Rich, A.; Jugder, B.E.; Jayasena, T.; Inestrosa, N.C.; Sachdev, P.S. Identification of Cerebral Metal Ion Imbalance in the Brain of Aging Octodon degus. *Front. Aging Neurosci.* **2017**, *9*, 66. [[CrossRef](#)]
51. Lu, L.N.; Qian, Z.M.; Wu, K.C.; Yung, W.H.; Ke, Y. Expression of Iron Transporters and Pathological Hallmarks of Parkinson’s and Alzheimer’s Diseases in the Brain of Young, Adult, and Aged Rats. *Mol. Neurobiol.* **2017**, *54*, 5213–5224. [[CrossRef](#)]
52. Takahashi, S.; Takahashi, I.; Sato, H.; Kubota, Y.; Yoshida, S.; Muramatsu, Y. Age-related changes in the concentrations of major and trace elements in the brain of rats and mice. *Biol. Trace Elem. Res.* **2001**, *80*, 145–158. [[CrossRef](#)]
53. Hidalgo, J.; Penkowa, M.; Giralto, M.; Carrasco, J.; Molinero, A. Metallothionein expression and oxidative stress in the brain. In *Methods in Enzymology*; Academic Press: Cambridge, MA, USA, 2002; Volume 348, pp. 238–249. [[CrossRef](#)]
54. West, A.K.; Hidalgo, J.; Eddins, D.; Levin, E.D.; Aschner, M. Metallothionein in the central nervous system: Roles in protection, regeneration and cognition. *Neurotoxicology* **2008**, *29*, 489–503. [[CrossRef](#)]
55. Suzuki, K.; Nakajima, K.; Kawaharada, U.; Hara, F.; Uehara, K.; Otaki, N.; Kimura, M.; Tamura, Y. Localization of metallothionein in the brain of Macaca fascicularis. *Acta Histochem. Cytochem.* **1992**, *25*, 609–616. [[CrossRef](#)]
56. Nishimura, N.; Nishimura, H.; Ghaffar, A.; Tohyama, C. Localization of metallothionein in the brain of rat and mouse. *J. Histochem. Cytochem.* **1992**, *40*, 309–315. [[CrossRef](#)] [[PubMed](#)]
57. Young, J.K.; Garvey, J.S.; Huang, P.C. Glial immunoreactivity for metallothionein in the rat brain. *Glia* **1991**, *4*, 602–610. [[CrossRef](#)] [[PubMed](#)]
58. Masters, B.A.; Quaipe, C.J.; Erickson, J.C.; Kelly, E.J.; Froelick, G.J.; Zambrowicz, B.P.; Brinster, R.L.; Palmiter, R.D. Metallothionein III is expressed in neurons that sequester zinc in synaptic vesicles. *J. Neurosci.* **1994**, *14*, 5844–5857. [[CrossRef](#)] [[PubMed](#)]

59. Brellou, G.; Vlemmas, I.; Lekkas, S.; Papaioannou, N. Immunohistochemical investigation of amyloid beta-protein (Abeta) in the brain of aged cats. *Histol. Histopathol.* **2005**, *20*, 725–731. [[CrossRef](#)]
60. Head, E.; Moffat, K.; Das, P.; Sarsoza, F.; Poon, W.W.; Landsberg, G.; Cotman, C.W.; Murphy, M.P. Beta-amyloid deposition and tau phosphorylation in clinically characterized aged cats. *Neurobiol. Aging.* **2005**, *26*, 749–763. [[CrossRef](#)] [[PubMed](#)]
61. Gunn-Moore, D.A.; McVee, J.; Bradshaw, J.M.; Pearson, G.R.; Head, E.; Gunn-Moore, F.J. Ageing changes in cat brains demonstrated by beta-amyloid and AT8-immunoreactive phosphorylated tau deposits. *J. Feline Med. Surg.* **2006**, *8*, 234–242. [[CrossRef](#)]
62. Chambers, J.K.; Tokuda, T.; Uchida, K.; Ishii, R.; Tatebe, H.; Takahashi, E.; Tomiyama, T.; Une, Y.; Nakayama, H. The domestic cat as a natural animal model of Alzheimer’s disease. *Acta Neuropathol. Commun.* **2015**, *3*, 78. [[CrossRef](#)] [[PubMed](#)]
63. Thal, D.R.; Rüb, U.; Orantes, M.; Braak, H. Phases of A beta-deposition in the human brain and its relevance for the development of AD. *Neurology* **2002**, *58*, 1791–1800. [[CrossRef](#)]
64. Rossner, S.; Lange-Dohna, C.; Zeitschel, U.; Perez-Polo, J.R. Alzheimer’s disease beta-secretase BACE1 is not a neuron-specific enzyme. *J. Neurochem.* **2005**, *92*, 226–234. [[CrossRef](#)] [[PubMed](#)]
65. Leuba, G.; Wernli, G.; Vernay, A.; Kraftsik, R.; Mohajeri, M.H.; Saini, K.D. Neuronal and nonneuronal quantitative BACE immunocytochemical expression in the entorhinohippocampal and frontal regions in Alzheimer’s disease. *Dement. Geriatr. Cogn. Disord.* **2005**, *19*, 171–183. [[CrossRef](#)] [[PubMed](#)]
66. Jin, S.M.; Cho, H.J.; Kim, Y.W.; Hwang, J.Y.; Mook-Jung, I. Ab-induced Ca²⁺ influx regulates astrocytic BACE1 expression via calcineurin/NFAT4 signals. *Biochem. Biophys. Res. Commun.* **2012**, *425*, 649–655. [[CrossRef](#)]
67. Orre, M.; Kamphuis, W.; Osborn, L.M.; Jansen, A.H.P.; Kooijman, L.; Bossers, K.; Hol, E.M. Isolation of glia from Alzheimer’s mice reveals inflammation and dysfunction. *Neurobiol. Aging* **2014**, *35*, 2746–2760. [[CrossRef](#)] [[PubMed](#)]
68. Zhao, J.; O’Connor, T.; Vassar, R. The contribution of activated astrocytes to Ab production, implications for Alzheimer’s disease pathogenesis. *J. Neuroinflamm.* **2011**, *8*, 150. [[CrossRef](#)]
69. Blasko, I.; Veerhuis, R.; Stampfer-Kountchev, M.; Saurwein-Teissl, M.; Eikelenboom, P.; Grubeck-Loebenstien, B. Costimulatory effects of interferon-g and interleukin-1b or tumor necrosis factor a on the synthesis of Ab1–40 and Ab1–42 by human astrocytes. *Neurobiol. Dis.* **2000**, *7*, 682–689. [[CrossRef](#)] [[PubMed](#)]
70. Borrás, D.; Ferrer, I.; Pumarola, M. Age related changes in the brain of the dog. *Vet. Pathol.* **1999**, *36*, 202–211. [[CrossRef](#)]
71. Gavier-Widen, D.; Wells, G.A.; Simmons, M.M.; Wilesmith, J.W.; Ryan, J. Histological observations on the brains of symptomless 7-year-old cattle. *J. Comp. Pathol.* **2001**, *124*, 52–59. [[CrossRef](#)]
72. Capucchio, M.T.; Marquez, M.; Pregel, P.; Foradada, L.; Bravo, M.; Mattutino, G.; Torre, C.; Schiffer, D.; Catalano, D.; Valenza, F.; et al. Parenchymal and vascular lesions in ageing equine brains, histological and immunohistochemical studies. *J. Comp. Pathol.* **2010**, *142*, 61–73. [[CrossRef](#)]
73. Leskovjan, A.C.; Kretlow, A.; Lanzirrotti, A.; Barrea, R.; Vogt, S.; Miller, L.M. Increased brain iron coincides with early plaque formation in a mouse model of Alzheimer’s disease. *Neuroimage* **2011**, *55*, 32–38. [[CrossRef](#)]

Disclaimer/Publisher’s Note: The statements, opinions and data contained in all publications are solely those of the individual author(s) and contributor(s) and not of MDPI and/or the editor(s). MDPI and/or the editor(s) disclaim responsibility for any injury to people or property resulting from any ideas, methods, instructions or products referred to in the content.